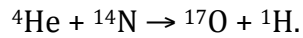


Chapter 10 NUCLEAR REACTIONS

10.1 Introduction

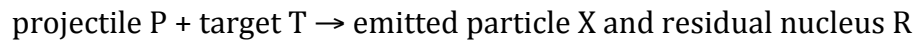
The study of nuclear reactions is important for a number of reasons. Progress in the understanding of nuclear reactions has occurred at a faster pace and generally a higher level of sophistication has been achieved compared to similar studies of chemical reactions. The approaches used to understand nuclear reactions are of value to any chemist who wishes a deeper insight into chemical reactions. There are certain nuclear reactions that play a preeminent role in the affairs of man and our understanding of the natural world in which we live. For example, life on earth would not be possible without the energy provided to us by the sun. That energy is the energy released in the nuclear reactions that drive the sun and other stars. For better or worse, the nuclear reactions, fission and fusion, are the basis for nuclear weapons, which have shaped much of the geopolitical dialog for the last 50 years. Apart from the intrinsically interesting nature of these dynamic processes, their practical importance would be enough to justify their study.

To discuss nuclear reactions effectively we must understand the notation or jargon that is widely used to describe them. Let us begin by considering the nuclear reaction

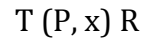


Most nuclear reactions are studied by inducing a collision between two nuclei where one of the reacting nuclei is at rest (the *target* nucleus) while the other nucleus (the

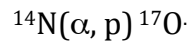
projectile nucleus) is in motion. (Exceptions to this occur both in nature and in the laboratory in studies where both the colliding nuclei are in motion relative to one another). But let us stick to the scenario of a moving projectile and a stationary target nucleus. Such nuclear reactions can be described generically as



For example, the first reaction discussed above might occur by bombarding ^{14}N with alpha particles to generate an emitted particle, the proton and a residual nucleus ^{17}O . A shorthand way to denote such reactions is, for the general case,

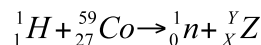


or for the specific example



In a nuclear reaction, there is conservation of the number of protons and neutrons (and thus the number of nucleons). Thus the total number of neutrons (protons) on the left and right sides of the equations must be equal.

Sample Problem. Consider the reaction $^{59}\text{Co}(p, n)$. What is the product of the reaction?



On the left side of the equation we have $27 + 1$ protons. On the right side we have $0 + X$ protons where X is atomic number of the product. Obviously $X=28$ (Ni). On the left hand side, we have $59 + 1$ nucleons and on the right side, we must have $1 + Y$ nucleons where $Y=59$. So the product is ^{59}Ni .

There is also conservation of energy, momentum, angular momentum and parity, which will be discussed below.

10.2 Energetics of Nuclear Reactions

Consider the $T(P, x)R$ reaction. Neglecting electron binding energies, we have, for the energy balance in the reaction,

$$m_P c^2 + T_P + m_T c^2 = m_R c^2 + T_R + m_x c^2 + T_x$$

where T_i is the kinetic energy of the i^{th} particle and m_i represents the mass-energy of the i^{th} species. (Note that since R and x may be formed in an excited state, the values of m may be different than the ground state masses.)

The *Q value* of the reaction is defined as the difference in mass energies of the product and reactants, *i.e.*,

$$Q = [m_p + m_T - (m_x + m_R)]c^2 = T_x + T_R - T_P$$

Note that if Q is positive, the reaction is **exoergic** while if Q is negative, the reaction is **endoergic**. Thus the sign convention for Q is exactly the opposite of the familiar ΔH in chemical reactions. A necessary *but not sufficient* condition for the occurrence of a nuclear reaction is that

$$Q + T_P > 0.$$

Q is an important quantity for nuclear reactions. If the masses of both the products and reactants are known (see Appendices), the Q value can be calculated using the mass excess, Δ , as

$$Q = \Delta(\text{projectile}) + \Delta(\text{target}) - \sum \Delta(\text{products})$$

It can be measured by measuring the masses or kinetic energies of the reactants and products in a nuclear reaction. However, we can show, using conservation of

momentum, that only T_x and the angle θ of x with respect to the direction of motion of P suffice to determine Q.

In the laboratory system, a typical nuclear collision can be depicted as shown in Figure 10-1. Conserving momentum in the x direction, we can write

$$m_P v_P = m_x v_x \cos \theta + m_R v_R \cos \phi$$

Applying conservation of momentum in the y direction, we have

$$0 = -m_x v_x \sin \theta + m_R v_R \sin \phi$$

where m_i and v_i are the mass and velocity of the i^{th} species. If we remember that the momentum $p = mv = (2mT)^{1/2}$, we can substitute in the above equation as

$$(m_P T_P)^{1/2} - (m_x T_x)^{1/2} \cos \theta = (m_R T_R)^{1/2} \cos \phi$$

$$(m_x T_x)^{1/2} \sin \theta = (m_R T_R)^{1/2} \sin \phi$$

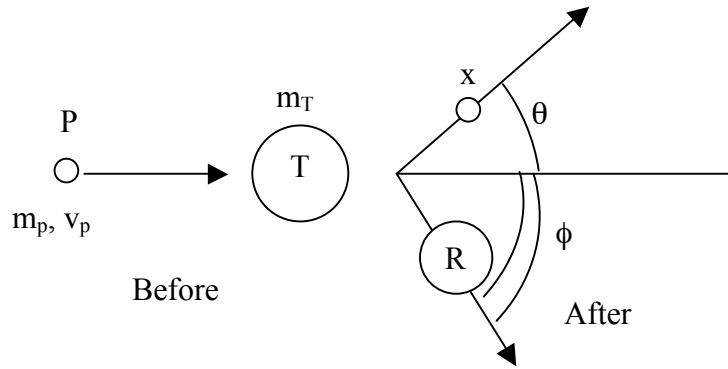


Figure 10-1. Schematic diagram of a nuclear reaction.

Squaring and adding the equations, we have

$$m_P T_P - 2 (m_P T_P m_x T_x)^{1/2} \cos \theta + m_x T_x = m_R T_R$$

Previously we had said that

$$Q = T_x - T_P - T_R$$

Plugging in this definition of Q, the value of T_R , we have just calculated, we get

$$Q = T_x \left(1 + \frac{m_x}{m_R} \right) - T_p \left(1 - \frac{m_p}{m_R} \right) - \frac{2}{m_R} (m_p T_p m_x T_x)^{1/2} \cos\theta$$

This is the all-important *Q equation*. What does it say? It says that if we measure the kinetic energy of the emitted particle x and the angle at which it is emitted in a reaction, and we know the identities of the reactants and products of the reactions, we can determine the Q value of the reaction. In short, we can measure the energy release for any reaction by measuring the properties of one of the products. If we calculate the Q value of a reaction using a mass table, then we can turn this equation around to calculate the energy of the emitted particle using the equation

$$T_x^{1/2} = \frac{(m_p m_x T_p)^{1/2} \cos\theta \pm \{m_p m_x T_p \cos^2\theta + (m_R + m_x)m_R Q + (m_R - m_p)T_p\}}{m_R + m_x}^{1/2}$$

For additional insight, let us now consider the same reaction as described in the *center-of-mass (cm)* coordinate system. In the cm system the total momentum of the particles is zero, before and after the collisions. The reaction as viewed in the laboratory and cm system is shown in Figure 10-2.

A replacement figure is needed here with the same notation as used in the chapter

Figure 10-2. Schematic view of a nuclear reaction in the laboratory and cm systems.

The kinetic energy of the center of mass is

$$T_{cm} = (m_p + m_T)v_{cm}^2/2$$

where v_{cm} ($=v_p m_p / (m_p + m_T)$) is the speed of the center of mass. Substituting, in the above equation, we have

$$T_{cm} = \frac{1}{2}(m_p + m_T) \left[\frac{m_p v_p}{m_p + m_T} \right]^2 = \frac{1}{2} m_p v_p^2 \left(\frac{m_p}{m_p + m_T} \right) = T_{lab} \left(\frac{m_p}{m_p + m_T} \right)$$

where T_{lab} is the kinetic energy in the lab system before the reaction, *i.e.*,

$$T_{lab} = \frac{1}{2} m_p v_p^2$$

The kinetic energy carried in by the projectile, T_{lab} , is not fully available to be dissipated in the reaction. Instead, an amount T_{cm} , must be carried away by the center of mass. Thus the available energy to be dissipated is $T_{lab} - T_{cm} \equiv T_0 = [M_T / (M_T + M_p)] T_{lab}$. The energy available for the nuclear reaction is $Q + T_0$. To make the reaction go, the sum $Q + T_0$ must be greater than or equal to zero. Thus, rearranging a few terms, the condition for having the reaction occur is that

$$T_p \geq -Q(m_p + m_T)/m_T$$

This minimum kinetic energy that the projectile must have to make the reaction go is called the *threshold energy* for the reaction.

Sample Problem: Consider the $^{14}\text{N}(\alpha, p)^{17}\text{O}$ reaction. What is the threshold energy for this reaction?

$$Q = (m_\alpha + m_N - (m_p + m_O))c^2 = 2.425 + 2.863 - 7.289 - (-0.809) = -1.19 \text{ MeV}$$

$$T_\alpha = -(-1.19)(4 + 14)/14 = 1.53 \text{ MeV}$$

10.3 Reaction types and mechanisms

Nuclear reactions, like chemical reactions, can occur via different reaction mechanisms. Weisskopf has presented a simple conceptual model (Figure 10-3) for illustrating the relationships between the various nuclear reaction mechanisms.

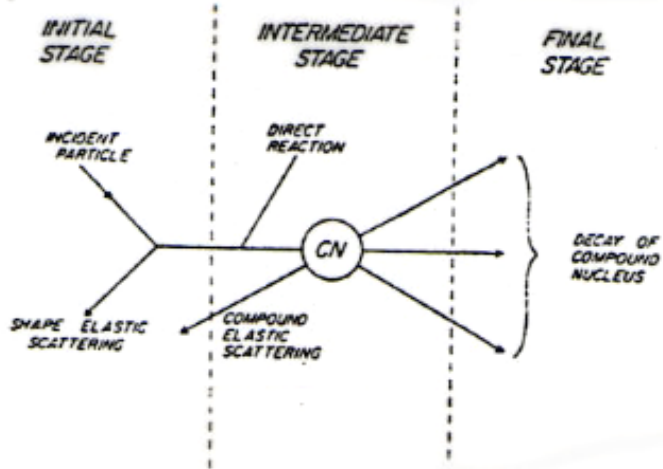


Figure 10-3. A conceptual view of the stages of a nuclear reaction (after V.F.Weisskopf, Rev. Mod. Phys. **29**, 174 (1959)).

Consider a general nuclear reaction of the type $A(a, b)B$ bearing in mind that for some cases, the nuclei b and B may be identical to a and A . As the projectile a moves near the target nucleus A , it will have a certain probability of interacting with the nuclear force field of A causing it to change direction but not to lose any energy. ($Q=0$) (Figure 10-3). This reaction mechanism is called *shape elastic scattering*. If shape elastic scattering doesn't occur, then the projectile may interact with A via a two body collision between the projectile and some nucleon of A , raising the nucleon of A to an unfilled level. (Figure 10-3). If the struck nucleon leaves the nucleus, a *direct reaction* is said to have occurred. If the struck nucleon does not leave the nucleus, further two-body collisions may occur and eventually the entire kinetic energy of the projectile nucleus may be distributed between the nucleons of the $a +$

A combination leading to the formation of a *compound nucleus C* (see Figure 10-3).

Because of the complicated set of interactions leading to the formation of the compound nucleus, loosely speaking, it ‘forgets’ its model of formation and its subsequent breakup only depends on the excitation energy, angular momentum of *C*, etc., and not the nature of the projectile and target nuclei. Sometimes the compound nucleus may emit a particle of the same kind as the projectile (or even the projectile itself) with the same energy as the projectile had. If this happens, we say *compound elastic scattering* has occurred. Also *C* may decay into reaction products that are unlike the projectile or target nuclei. We shall spend much of this chapter discussing these reaction mechanisms and some others not yet mentioned. But before doing so, let us see what general properties of nuclear reactions we can deduce from relatively simple arguments.

10.4 Nuclear reaction cross sections.

Consider the situation (Figure 10-4) where a beam of projectile nuclei of intensity ϕ_0 particles/sec is incident upon a thin foil of target nuclei with the result that the beam is attenuated by reactions in the foil such that the transmitted intensity is ϕ particles/sec.

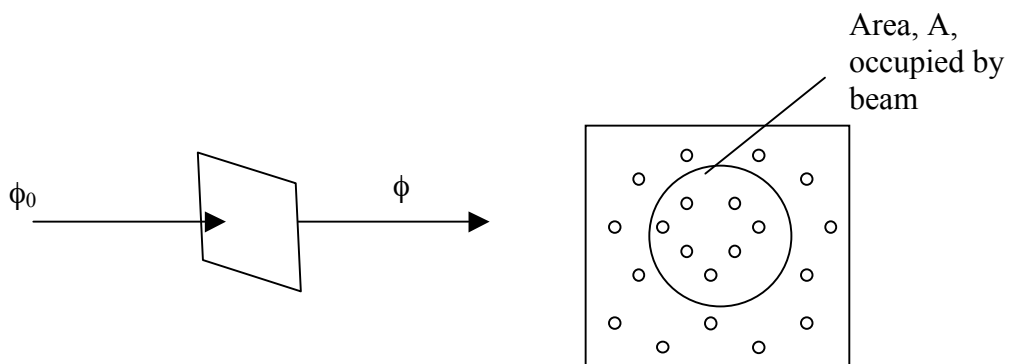


Figure 10-4. Schematic diagram showing the attenuation of an incident projectile beam.

We can ask what fraction of the incident particles disappear from the beam, i.e., react, in passing through the foil. Let us assume the beam intersects an area A on the foil. We can then assert that the fraction of beam particles that is blocked (reacts) is the fraction of the area A that is covered by target nuclei. If the foil contains N atoms/cm², then the area a that is covered by nuclei is $N(\text{atoms}/\text{cm}^2) \times A (\text{cm}^2)$ x (the effective area subtended by one atom) (cm²/atom). This latter term, the effective area subtended by one atom, is called the *cross section*, σ , for the reaction under study. Then the fraction of the area A that is blocked is a/A or $N(\text{atoms}/\text{cm}^2)\sigma(\text{cm}^2/\text{atom})$. If we say the number of projectile nuclei absorbed per unit time is $\Delta\phi$, then we have

$$\Delta\phi = -\phi N\sigma$$

As an aside, we note the units of N are atoms/cm² or thickness, Δx (cm) x density $n(\text{atoms}/\text{cm}^3)$. Expressing the above equation as a differential equation, we have

$$-\frac{d\phi}{\phi} = \phi N \sigma$$

Thus, upon rearranging, we have

$$\frac{d\phi}{\phi} = -N\sigma dx$$

$$\int_{\phi_{initial}}^{\phi_{trans}} \frac{d\phi}{\phi} = -n\sigma \int_0^x dx$$

$$\ln \frac{\phi_{trans}}{\phi_{initial}} = -n\sigma x$$

$$\phi_{trans} = \phi_{initial} e^{-n\sigma x}$$

Thus we see exponential absorption of the incident projectile beam (and have thus derived a form of the Lambert-Beers Law). The number of reactions that are occurring is the difference between the initial and transmitted flux, *i.e.*,

$$\phi_{\text{initial}} - \phi_{\text{trans}} = \phi_{\text{initial}} (1 - \exp(-n\sigma x))$$

The foregoing discussion focusses on the attenuation of the incident beam and thus refers to *all* reactions. In many cases, we are interested in only one of several reactions that may be taking place. We can refer to the cross section for that particular reaction. In addition, we may be interested not only in a specific product, but a particular product moving in a particular direction relative to the direction of the projectile beam (see Figure 10-5 for a sketch of a typical experimental measurement).

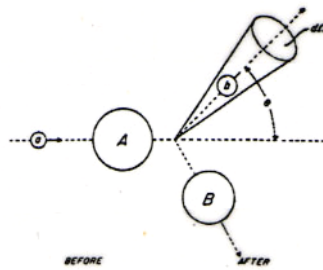


Figure 10-5. Schematic diagram of a typical experimental setup.

In this case, we can speak of a *differential cross section*, or the cross section per unit solid angle, $d\sigma/d\Omega$. For a thin target, we have

$$dN/d\Omega = \phi n (d\sigma/d\Omega) dx$$

where $dN/d\Omega$ is the number of particles detected moving in a particular direction per unit solid angle. The total cross section, σ , is given as

$$\sigma = \iint_0^{2\pi} \frac{d\sigma}{d\Omega}(\theta) \sin \theta d\theta d\phi$$

The description given above is appropriate for work at accelerators, where one has a beam of particles that is smaller than the target. In this case, the beam intensity, ϕ is given in particles/sec and the target density, N , is given in atoms/cm². In a nuclear reactor, we immerse a small target in a sea of neutrons. In this case, the neutron flux, ϕ , represents the number of neutrons passing through the target per cm² per sec and N is the total number of atoms in the target. Otherwise the arithmetic is the same. For charged particles from an accelerator, the beam intensity is usually measured as a current. Thus for a beam of protons with a current of 1 μ ampere, we have

$$\phi = (1 \mu\text{ampere}) (10^{-6} \text{ Coul/sec}/\mu\text{ampere}) \left(\frac{1}{1.602 \times 10^{-19} \text{ Coul/proton}} \right) = 6.24 \times 10^{12} \text{ protons/sec}$$

For a beam of some other ion with charge q , one simply divides by the charge on the ion to get the projectile beam intensity. Thus, for a beam of 4 μ amperes of Ar⁺¹⁷ ions, we have

$$\phi = (4 \times 10^{-6} \text{ Coul/sec}) \left(\frac{1}{17 \times 1.602 \times 10^{-19} \text{ Coul/Ar}} \right) = 1.47 \times 10^{12} \text{ Ar/sec}$$

To put the intensities of beams of differing charges on a common footing, it is common to quote charge particle beam intensities in units of *particle microamperes* or *particle nanoamperes* where 1 particle microampere = 6.24×10^{12} ions/sec.

It is easy to calculate the number of product nuclei produced during an irradiation, N . If we assume the product nuclei are stable, then the number of nuclei produced is the (rate of production) \times (length of the irradiation, t). For a thick target irradiation, we have

$$N = \phi(1 - \exp(-n\sigma\Delta x))t$$

For a thin target if we expand $(1 - \exp(-n\sigma\Delta x))$, we have

$$N = \phi n \sigma \Delta x t$$

But, what if the products are radioactive? Then some of them will decay during the irradiation. In this case, we can setup the familiar differential equations

$$\frac{dN}{dt} = (\text{rate of production}) - (\text{rate of decay})$$

$$\frac{dN}{dt} = n\sigma\Delta x\phi - \lambda N$$

$$\frac{dN}{(n\sigma\Delta x\phi - \lambda N)} = dt$$

Multiplying by λ and rearranging

$$\frac{d(\lambda N)}{\lambda N - n\sigma\Delta x\phi} = -\lambda dt$$

Integrating, we have

$$\ln(\lambda N - n\sigma\Delta x \phi) \Big|_0^N = -\lambda t \Big|_0^t$$

$$\frac{N\lambda - n\sigma\Delta x \phi}{-n\sigma\Delta x \phi} = e^{-\lambda t}$$

$$A = \Delta N = n \rightarrow \Delta x \big(1 - e^{-\lambda t}\big)$$

where A is the disintegration rate of product nuclei at the end of the irradiation. The number of product nuclei, N , present at the end of the irradiation is A/λ or

$$N = \frac{n\sigma\Delta x \phi}{\lambda} \left(1 - e^{-\lambda t}\right)$$

This relationship is shown in Figure 10-6.

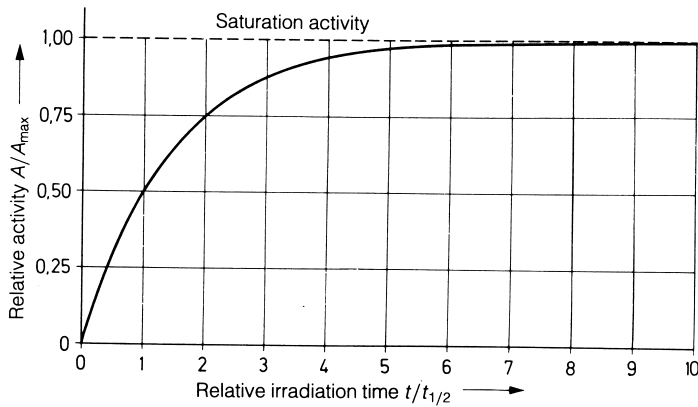


Figure 10-6. Variation of product activity during an irradiation. From Lieser.

Note that in the limit of infinitely long irradiation, $e^{-\lambda t} \rightarrow 0$, and thus the activity present is $n\sigma\Delta x\phi$ which is termed the *saturation activity*. Note also that for very short times (compared to the half-life of the product nuclei), $e^{-\lambda t} \rightarrow 1 - \lambda t + \dots$ Thus the activity increases linearly with time. In general, we note that we achieve 1/2 the saturation activity after an irradiation of one half-life, 3/4 of the saturation activity after irradiating two half-lives, 7/8 of the saturation activity after irradiating 3 half-lives, etc. Thus it does not pay to make the irradiation longer than 1-2 half-lives. (This effect can be used to tune the length of the irradiation to maximize the yield of the product of interest relative to the other reaction products)

Sample Problem

Calculate the activity of ^{254}No ($t_{1/2} = 55$ s) produced in a one-minute irradiation of ^{208}Pb by ^{48}Ca . Assume the ^{208}Pb target thickness is 0.5 mg/cm^2 , the ^{48}Ca beam current is $0.5 \text{ particle microamperes}$ and the $^{208}\text{Pb}(^{48}\text{Ca}, 2n)$ reaction cross section is $3.0 \mu\text{b}$.

Solution:

$$A = N\sigma\phi(1 - e^{-\lambda t_i})$$

$$N = (0.5 \times 10^{-3} \text{ g/cm}^2)(6.02 \times 10^{23} \text{ atoms/g-at-wt})/208 \text{ g/g-at-wt} = 1.44 \times 10^{18}$$

$$\text{atoms/cm}^2$$

$$\sigma = 3 \times 10^{-30} \text{ cm}^2$$

$$\phi = (0.5 \times 10^{-6} \text{ Coulombs/sec})/1.602 \times 10^{-19} \text{ Coulombs/ion} = 3.12 \times 10^{12} \text{ ions/sec}$$

$$t_i = 60 \text{ sec}$$

$$\lambda = (\ln 2)/55 \text{ sec} = 1.26 \times 10^{-2} \text{ sec}^{-1}$$

$$A = 7.2 \text{ dis/sec}$$

Let us consider what we can learn about cross sections from some general considerations. Consider the reaction of an uncharged particle (a neutron) with a nucleus as shown in Figure 10-7.

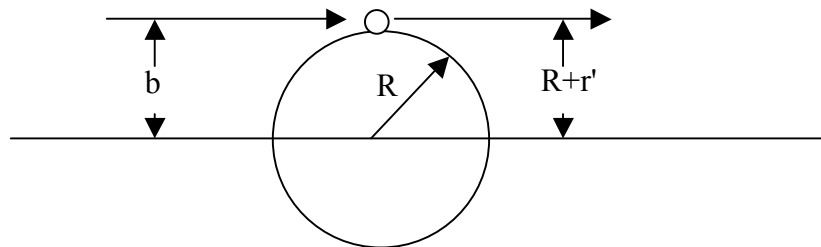


Figure 10-7. Schematic diagram of a grazing collision of a neutron with a nucleus.

The neutron makes a grazing collision with the nucleus. The impact parameter b is taken to be the sum of the radii of the projectile and target nuclei. Thus the cross section can be written as

$$\sigma \approx \pi(R + r')^2 = \pi r_0^2(A_P + A_T)^2$$

where r' is the radius of the projectile. Applying classical mechanics to this problem, we can write for the orbital angular momentum, ℓ ,

$$\ell = \vec{r} \times \vec{p} = pb$$

In quantum mechanics, $\ell \square \ell^\circ$, and the momentum, p, is given by

$$p = \frac{\hbar}{\lambda}$$

Thus we have

$$\ell \hbar = \frac{\hbar b}{\lambda}$$

$$b = \ell \lambda$$

This is not quite right because ℓ is quantized but b is not. We get around this by associating b with certain rings or zones on the target. (Figure 10-8) Figure 10-8 suggests that for head-on collisions ($\ell = 0$), the range of b is from 0 to λ while for $\ell = 1$ collisions, the range of b is from λ to 2λ . Thus the cross section is larger for larger impact parameters and these larger impact parameters are associated with larger angular momenta. We can write the cross section for a specific value of ℓ as

$$\sigma_\ell = \pi(\ell + 1)^2 \lambda^2 - \pi \ell^2 \lambda^2$$

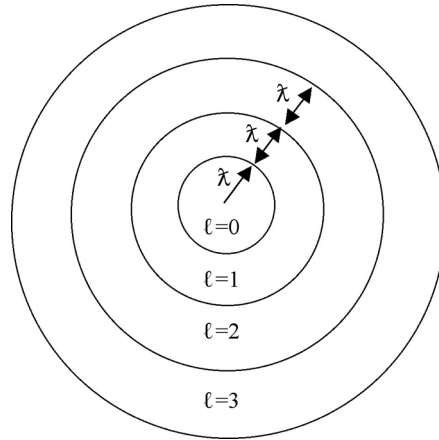


Figure 10-8. Schematic bulls-eye view of the target nucleus.

$$\sigma_\ell = \pi\hat{\lambda}^2(\ell^2 + 2\ell + 1 - \ell^2)$$

$$\sigma_\ell = \pi\hat{\lambda}^2(2\ell + 1)$$

The total reaction cross section is obtained by summing over all ℓ values as

$$\sigma_{total} = \sum_\ell \sigma_\ell = \sum_{\ell=0}^{\ell_{max}} \pi\hat{\lambda}^2(2\ell + 1) = \pi\hat{\lambda}^2 \sum_{\ell=0}^{\ell_{max}} (2\ell + 1) = \pi\hat{\lambda}^2 (\ell_{max} + 1)^2$$

We can write for the maximum angular momentum, ℓ_{max} ,

$$\ell_{max} = \frac{R}{\hat{\lambda}}$$

$$\ell_{\max} + 1 = \frac{R + \lambda}{\lambda}$$

Thus we have for the total cross section

$$\sigma_{total} = \pi(R + \lambda)^2$$

The total cross section is proportional to the size of the target nucleus and the “size” of the projectile nucleus. Since the wave length of the projectile, λ , goes to infinity as the projectile energy goes to zero, the cross sections for neutrons at low energies can be very large. The above discussion is based upon classical mechanics. We need to indicate how the problem would look if we used quantum mechanics to treat it. In quantum mechanics, we can write an similar expression for the total reaction cross section,

$$\sigma_{total} = \pi \lambda^2 \sum_{\ell=0}^{\infty} (2\ell + 1) T_\ell$$

where the transmission coefficient T_ℓ varies between 0 and 1. The transmission coefficient expresses the probability that a given angular momentum transfer ℓ will occur. At high projectile energies, $T_\ell = 1$ for $\ell \leq \ell_{\max}$ and $T_\ell = 0$ for $\ell \geq \ell_{\max}$. At very low projectile energies, $T_\ell = \varepsilon^{1/2}$ for $\ell=0$ and $T_\ell = 0$ for $\ell > 0$, where ε is the projectile energy. Thus, at very low energies, we have

$$\sigma_{total} \propto \pi \lambda^2 \sqrt{\epsilon} \propto \pi \frac{\hbar^2}{2m\epsilon} \sqrt{\epsilon} \propto \frac{1}{\sqrt{\epsilon}}$$

Such behavior of the cross sections for neutron induced reactions is referred to as '1/v' behavior.

Now let us consider the interaction of a charged particle with a nucleus as shown in Figure 10-9.

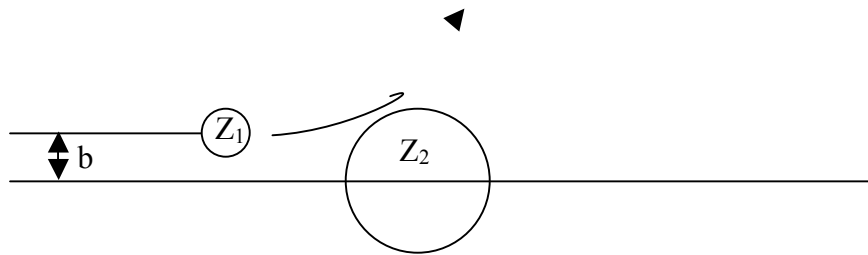


Figure 10-9 Schematic diagram of a charged particle induced reaction.

As the projectile approaches the target nucleus, it feels the long range Coulomb force and is deflected. As a consequence, the range of collisions corresponds to a smaller range of impact parameters. If the incident projectile has an energy ϵ at an infinite separation from the target nucleus, at the distance of closest approach R , it has a kinetic energy of $\epsilon - B$ where B , the Coulomb barrier, is given by

$$B = Z_1 Z_2 e^2 / R$$

At the point of closest approach, the momentum p of the projectile is $(2mT)^{1/2}$. Thus we can write

$$p = (2mT)^{1/2} = (2\mu)^{1/2} (\epsilon - B)^{1/2} = (2\mu\epsilon)^{1/2} (1 - B/\epsilon)^{1/2}$$

where μ is the reduced mass of the system ($=A_1A_2/(A_1 + A_2)$). Classically we have, for the orbital angular momentum,

$$\ell = \vec{r} \times \vec{p}$$

$$\ell_{\max} = R(2\mu\varepsilon)^{1/2} \left(1 - \frac{B}{\varepsilon}\right)^{1/2}$$

Quantum mechanically, we have $\ell \rightarrow \ell \hbar$. So we can write

$$\sigma_{total} = \pi\hat{\lambda}^2(\ell_{\max} + 1)^2 \approx \pi\hat{\lambda}^2\ell_{\max}^2 = \pi\hat{\lambda}^2R^2 \frac{2\mu\varepsilon}{\hbar^2} \left(1 - \frac{B}{\varepsilon}\right) = \pi\hat{\lambda}^2R^2 \frac{1}{\hat{\lambda}^2} \left(1 - \frac{B}{\varepsilon}\right)$$

$$\sigma_{total} = \pi R^2 \left(1 - \frac{B}{\varepsilon}\right)$$

Note this last classical expression is valid only when $\varepsilon > B$. The combined general properties of cross sections for charged and uncharged particles are shown in Figure 10-10.

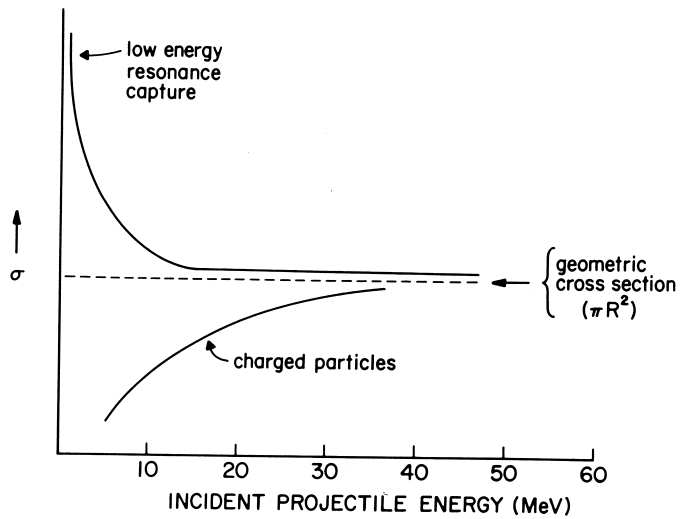


Figure 10-10 Near threshold behavior of neutron and charged particle induced reactions. From Ehmann and Vance.

Sample problem

Calculate the energy dependence of the total reaction cross section for the $^{48}\text{Ca} + ^{208}\text{Pb}$ reaction.

Solution:

$$\sigma_{total} = \pi R^2 \left(1 - \frac{B}{\varepsilon}\right)$$

$$R = R_{\text{Pb}} + R_{\text{Ca}} = 1.2 (208^{1/3} + 48^{1/3}) = 11.47 \text{ fm}$$

$$B = Z_1 Z_2 e^2 / R = (82)(20)(1.44 \text{ MeV-fm}) / 11.47 \text{ fm} = 205.9 \text{ MeV}$$

ε = energy of the projectile in the cm system

$\varepsilon(\text{MeV})$	$\sigma(\text{mb})$

208	41.7
210	80.7
220	264.9
230	433.1
240	587.2
250	729.1

Aside on barriers

In our semi-classical treatment of the properties of charged particle induced reaction cross sections, we have equated the reaction barrier B to the Coulomb barrier. That is, in reality, a simplification that is applicable to many but not all charged particle induced reactions.

The actual force (potential energy) felt by an incoming projectile is the sum of the nuclear, Coulomb and centrifugal forces (Figure 10.11). The Coulomb potential, $V_C(r)$ is approximated as the potential between a point charge Z_1e and a homogeneous charged sphere with charge Z_2e and radius R_C as

$$V_C(r) = Z_1Z_2/r \text{ for } r < R_C$$

$$V_C(r) = (Z_1Z_2/R_C) (3/2 - \frac{1}{2} (r^2/R_C^2)) \text{ for } r > R_C$$

The nuclear potential is frequently represented by a Woods-Saxon form (Chapter 5) as

$$V_{\text{nucl}}(r) = V_0/(1 + \exp((r-R/a)))$$

while the centrifugal potential is taken as

$$V_{cent}(r) = \frac{\hbar^2}{2\mu} \frac{\ell(\ell+1)}{r^2}$$

where $\ell\hbar$ is the orbital angular momentum of the incident projectile. The total potential, $V_{tot}(r)$, is the sum $V_C(r) + V_{nucl}(r) + V_{cent}(r)$. These different potentials are shown in Figure 10.11 using the $^{16}\text{O} + ^{208}\text{Pb}$ reaction as an example and input angular momenta of $\ell = 0, 10$, and $100\hbar$. Note that for the highest angular momentum, $\ell = 100\hbar$, the total potential is repulsive at all distances, *i.e.*, the ions don't fuse.

The actual ***interaction barrier***, is the value of $V_{total}(r)$ at the point when the colliding nuclei touch. That is slightly different from $V_C(r)$ at $r=R_C$, the ***Coulomb barrier***.

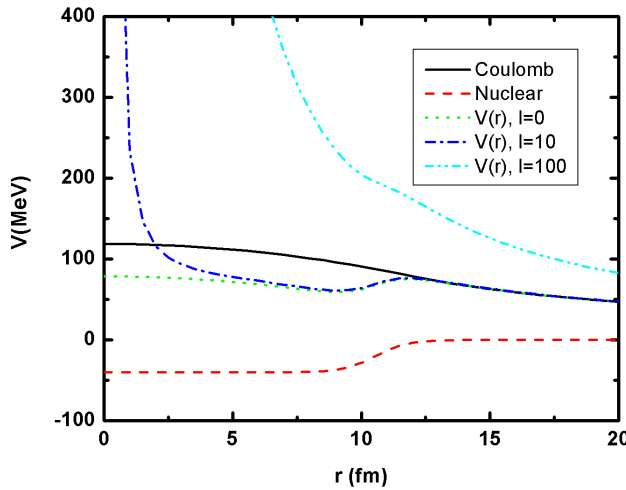


Figure 10.11 The nuclear, Coulomb, and total potentials for the interaction of ^{16}O with ^{208}Pb for various values of the orbital angular momentum.

10.5 Reaction observables

What do we typically measure when we study a nuclear reaction? We might measure σ_R , the total reaction cross section. This might be measured by a beam attenuation method ($\Phi_{\text{transmitted}}$ vs. Φ_{incident}) or by measuring all possible exit channels for a reaction where

$$\sigma_R = \sum_i^{b+B} \sigma_i(b, B)$$

We might measure the cross section for producing a particular product at the end of the reaction, $\sigma(Z, A)$. We might do this by measuring the radioactivity of the reaction products. We might, as discussed previously, measure the products emerging in a particular angular range, $d\sigma(\theta, \phi)/d\Omega$. This measurement is especially relevant for experiments with charge particle induced reactions where the incident beam provides a reference axis for θ and ϕ . The energy spectra of the emitted particles can be measured as $d\sigma/dE$ or we might observe the products emerging at a particular angle and with a particular energy, $d^2\sigma/dEd\Omega$.

10.6 Rutherford Scattering

One of the first possible outcomes of the collision of a charged particle with a nucleus is Rutherford or Coulomb scattering. The incident charged particle feels the long-range Coulomb force of the positively charged nucleus and is deflected from its path. (Figure 10-12).

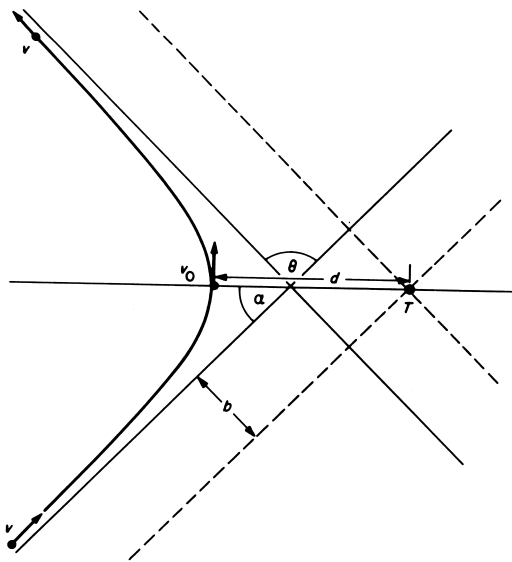


Figure 10-12 Schematic diagram of Rutherford scattering. From Satchler (1990).

The Coulomb force acting between a projectile of mass m , charge Z_1e and a target nucleus with charge Z_2e is given as

$$F_{coul} = \frac{Z_1 Z_2 e^2}{r^2}$$

where r is the distance between the projectile and target nuclei. The potential energy in this interaction is given as

$$PE = \frac{Z_1 Z_2 e^2}{r}$$

Consider a target nucleus that is much heavier than the projectile nucleus so that we can neglect the recoil of the target nucleus in the interaction. The projectile will follow a hyperbolic orbit, as shown in Figure 10-12 where b is the impact parameter, T_p is the kinetic energy of the projectile and d is the distance of closest

approach. At infinity, the projectile velocity is v . At $r=d$, the projectile velocity is v_0 .

Conservation of energy gives

$$\frac{1}{2}mv^2 = \frac{1}{2}mv_0^2 + \frac{Z_1Z_2e^2}{d}$$

Rearranging, we have

$$\left(\frac{v_0}{v}\right)^2 = 1 - \frac{d_0}{d}$$

where d_0 is given as

$$d_0 = \frac{2Z_1Z_2e^2}{mv^2} = \frac{Z_1Z_2e^2}{T_p}$$

If we now invoke the conservation of angular momentum, we can write

$$mvb = mv_0d$$

$$b^2 = \left(\frac{v_0}{v}\right)^2 d^2 = d(d - d_0)$$

It is a property of a hyperbola that

$$d = b \cot(\alpha/2)$$

Substituting from above, we have

$$\tan \alpha = 2b/d_0$$

Since $\theta = \pi - 2\alpha$, we can write

$$\cot\left(\frac{\theta}{2}\right) = \frac{2b}{d_0}$$

In Figure 10-13, we show the expected orbits of the projectile nuclei after undergoing Rutherford scattering for a typical case. Note that the most probable grazing trajectories result in projectiles

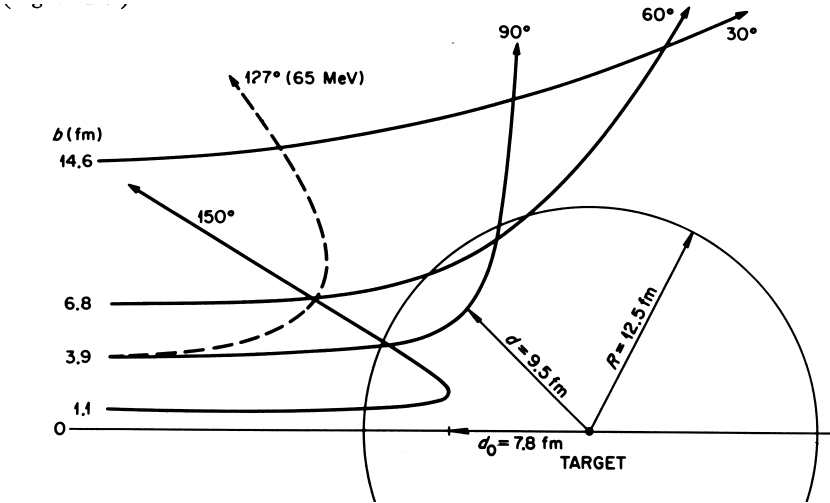


Figure 10-13. Diagram showing some representative projectile orbits for the interaction of 130 MeV ^{16}O with ^{208}Pb . [From Satchler (1990)].

being scattered to forward angles but that some head-on collisions result in large angle scattering. It was these latter events that led Rutherford to conclude that there was a massive object at the center of the atom.

We can make these observations more quantitative by considering the situation where a flux of I_0 particles/unit area is incident on a plane normal to the beam direction. The flux of particles passing through a ring of width db and with impact parameters between b and $b + db$ is given as

$$dI = (\text{Flux}/\text{unit area})(\text{area of ring})$$

$$dI = I_0 (2\pi b db)$$

Substituting from above, we have

$$dI = \frac{1}{4}\pi I_0 d_0^2 \frac{\cos\left(\frac{\theta}{2}\right)}{\sin^3\left(\frac{\theta}{2}\right)} d\theta$$

If we want to calculate the number of projectile nuclei that undergo Rutherford scattering into a solid angle $d\Omega$ at a plane angle θ , we can write

$$\frac{d\sigma}{d\Omega} = \frac{dI}{I_0} \frac{1}{d\Omega} = \left(\frac{d_0}{4}\right)^2 \frac{1}{\sin^4\left(\frac{\theta}{2}\right)} = \left(\frac{Z_1 Z_2 e^2}{4T_p^{cm}}\right)^2 \frac{1}{\sin^4\left(\frac{\theta}{2}\right)}$$

if we remember that

$$d\Omega = 2\pi \sin\theta d\theta$$

Note the strong dependence of the Rutherford scattering cross section upon scattering angle. Remember that Rutherford scattering is not a nuclear reaction, as it does not involve the nuclear force, only the Coulomb force between the charged nuclei. Remember that Rutherford scattering will occur to some extent in all studies of charged particle induced reactions and will furnish a "background" of scattered particles at forward angles.

Sample calculation:

Calculate the differential cross section for the Rutherford scattering of 215 MeV (lab energy) ^{48}Ca from ^{208}Pb at an angle of 20° .

$$\frac{d\sigma}{d\Omega} = \left(\frac{Z_1 Z_2 e^2}{4T_p^{cm}}\right)^2 \frac{1}{\sin^4\left(\frac{\theta}{2}\right)}$$

$$T_p^{cm} = 215 \times \frac{208}{256} = 174.7 \text{ MeV}$$

$$\frac{d\sigma}{d\Omega} = \left(\frac{20 \times 82 \times 1.44}{4 \times 174.7} \right)^2 \frac{1}{\sin^4\left(\frac{\theta}{2}\right)} = 12562 f \text{ fm}^2 = 125.6 b$$

10.7 Elastic (Diffractive) Scattering

Suppose we picture the interaction of the incident projectile nucleus with the target nucleus as it undergoes shape elastic scattering. It is convenient to think of this interaction as that of a plane wave with the nucleus as depicted in Figure 10-13.

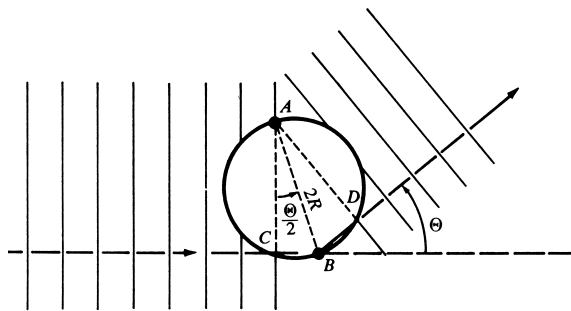


Figure 10-14. Schematic diagram of the interaction of a plane wave with the nucleus. [From Meyerhof (1967)].

Imagine further that all interactions take place on the nuclear surface. Assume that only points A and B on the nucleus scatter particles and that all other points absorb them. To get constructive interference between the incoming and outgoing wave we must fulfill the condition that

$$CB + BD = n\lambda$$

where λ is the wave length of the incident particle and n is an integer. Hence peaks should occur in the scattering cross section when

$$n\lambda = 2 \cdot 2R \cdot \sin\left(\frac{\theta}{2}\right)$$

In Figure 10-15, we show the angular distribution for the elastic scattering of 800 MeV protons from ^{208}Pb . The de Broglie wave length of the projectile is 0.85 fm while the nuclear radius R is about 7.6 fm ($1.28(208)^{1/3}$). We expect peaks ($n=2,3,4\dots$) with a spacing between them, $\Delta\theta$, of

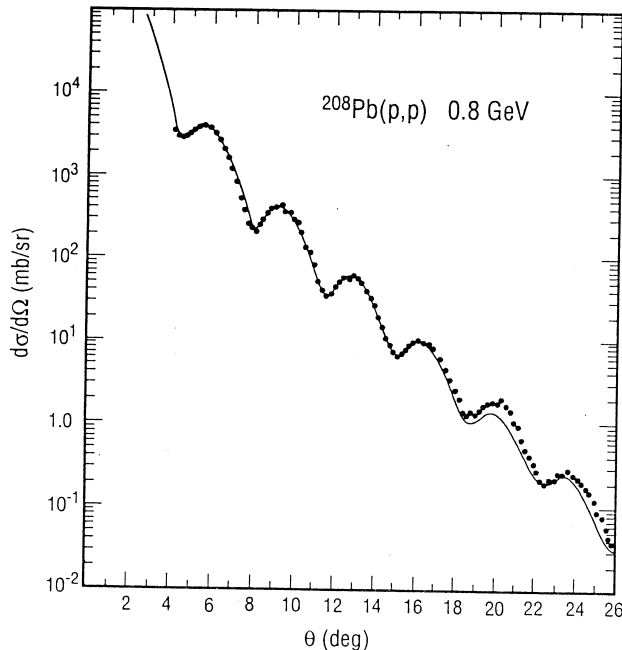


Figure 10-15. Angular distribution of 800 MeV protons that have been elastically scattered from ^{208}Pb . (G.S. Blanpied et al., Phys. Rev. C **18**, 1436 (1978))
3.2° while one observes a spacing of 3.5°. (This example is taken from G.F. Bertsch and E. Kashy, Am. J. Phys. **61**, 858 (1993).)

Aside on the optical model

The optical model is a tool to understand and parameterize studies of elastic scattering. It likens the interaction of projectile and target nucleus with that of a beam of light interacting with a glass ball. To simulate the occurrence of both elastic scattering and absorption (reactions) in the interaction, the glass ball is imagined to be somewhat cloudy.

In formal terms, the nucleus is represented by a nuclear potential that has a real and an imaginary part.

$$U_{\text{nucl}}(r) = V(r) + iW(r)$$

where the imaginary potential $W(r)$ describes absorption (reactions) as the depletion of flux into non-elastic channels and the real potential $V(r)$ describes the elastic scattering. Frequently the nuclear potential is taken to have the Woods-Saxon form

$$U_{\text{nucl}}(r) = -V_0 f_R(r) - iW_0 f_I(r)$$

where

$$f_{R,I}(r) = \left[1 + \exp\left(\frac{r - R_{R,I}}{a_{R,I}}\right) \right]^{-1}$$

The potential is thus described in terms of six parameters, the potential depths, V_0 , W_0 ; the radii R_R , R_I ; and the surface diffuseness a_R , a_I . By solving the Schrödinger equation with this nuclear potential (along with the Coulomb and centrifugal potentials), one can predict the cross section for elastic scattering, the angular distribution for elastic scattering and the total reaction cross section. The meaning of the imaginary potential depth W can be understood by noting that the mean free path of a nucleon in the nucleus, Λ , can be given as

$$\Lambda = \frac{v\hbar}{2W_0}$$

where v is the relative velocity. By fitting measurements of elastic scattering cross sections and angular distributions over a wide range of projectiles, targets and beam energies, one might hope to gain a universal set of parameters to describe elastic scattering (and the nuclear potential). That hope is only partially realized because only the tail of the nuclear potential affects elastic scattering and there are families of parameters that fit the data equally well, as long as they agree in the exterior regions of the nucleus.

10.8 Direct Reactions

As we recall from our general description of nuclear reactions, a *direct reaction* is said to occur if one of the participants in the initial two-body interaction involving the incident projectile leaves the nucleus. Generally speaking, these direct

reactions are divided into two classes, the *stripping reactions* in which part of the incident projectile is “stripped away” and enters the target nucleus and the *pickup reactions* in which the outgoing emitted particle is a combination of the incident projectile and a few target nucleons.

Let us consider stripping reactions first and in particular, the most commonly encountered stripping reaction, the (d, p) reaction. Formally the result of a (d, p) reaction is to introduce a neutron into the target nucleus and thus this reaction should bear some resemblance to the simple neutron capture reaction. But because of the generally higher angular momenta associated with the (d, p) reaction, there can be differences between the two reactions. Consider the A (d, p) B* reaction where the recoil nucleus B is produced in an excited state B*. We sketch out a simple picture of this reaction and the momentum relations in Figure 10-15.

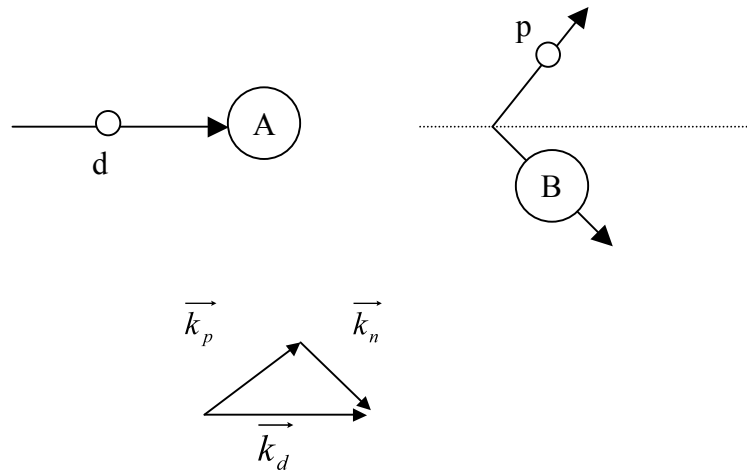


Figure 10-16 Sketch of a (d, p) reaction and the associated momentum triangle.

The momentum diagram for the reaction shown in Figure 10-16 assumes the momentum of the incident deuteron is $k_d \hbar$, the momentum of the emitted proton is

$k_p \hbar$ while $k_n \hbar$ is the momentum of the stripped neutron. From conservation of momentum, we have

$$k_n^2 = k_d^2 + k_p^2 - 2k_d k_p \cos\theta$$

If the neutron is captured at impact parameter R, the orbital angular momentum transferred to the nucleus, $\ell_n \hbar$, is given by

$$\ell_n \hbar = \vec{r} \times \vec{p} = R k_n \hbar$$

$$\ell_n = R k_n$$

Since we have previously shown that k_n is a function of the angle θ , we can now associate each orbital angular momentum transfer in the reaction with a given angle θ corresponding to the direction of motion of the outgoing proton. Thus the (d, p) reaction becomes a very powerful spectroscopic tool. By measuring the energy of the outgoing proton, we can deduce the Q value of the reaction and thus the energy of any excited state of the residual nucleus that is formed. From the direction of motion of the proton, we can deduce the orbital angular momentum transfer in the reaction, ℓ_n . If we know the ground state spin and parity of the residual nucleus, we can deduce information about the spin and parity of the excited states of the residual nucleus using the rules

$$||(|J_A - \ell_n| - 1/2)|| \leq J_{B^*} \leq J_A + \ell_n + 1/2$$

$$\pi_A \pi_{B^*} = (-1)^{\ell_n}$$

Other stripping reactions are reactions like (α , t), (α , d), etc. Typical pickup reactions are (p, d), (p, t), (α , ${}^6\text{Li}$), etc.

Sample Problem:

Calculate the angle at which the (d, p) cross section has a maximum for $\ell = 0, 1, 2, 3$ and 4. Assume a deuteron energy of 7 MeV and a proton energy of 13 MeV.

Use $R = 6$ fm.

$$k_d = 0.82 \text{ fm}^{-1}$$

$$k_p = 0.79 \text{ fm}^{-1}$$

$$k_n = \frac{\ell}{R}$$

Thus for $\ell = 0, 1, 2, 3, 4$, $k_n = 0, 0.17 \text{ fm}^{-1}, 0.33 \text{ fm}^{-1}, 0.50 \text{ fm}^{-1}, 0.67 \text{ fm}^{-1}$. Solving the momentum triangle,

$$\cos \theta = \frac{-k_n^2 + k_d^2 + k_p^2}{2k_d k_p}$$

$$\theta = 0^\circ, 12^\circ, 24^\circ, 36^\circ, 49^\circ \text{ for } \ell = 0, 1, 2, 3, 4$$

(A somewhat more correct expression would say $k_n R = [\ell(\ell+1)]^{1/2}$).

10.9 Compound Nucleus Reactions

The compound nucleus is a relatively long-lived reaction intermediate that is the result of a complicated set of two body interactions in which the energy of the projectile is distributed among all the nucleons of the composite system. How long does the compound nucleus live? From our definition above, we can say the compound nucleus must live for at least several times the time it would take a nucleon to traverse the nucleus (10^{-22} seconds). Thus the time scale of compound nuclear reactions is of the order of $10^{-18} - 10^{-16}$ sec. Lifetimes as long as 10^{-14} sec

have been observed. These relatively long times should be compared to the typical time scale of a direct reaction of 10^{-22} sec.

Another important feature of compound nucleus reactions is the mode of decay of the compound nucleus is independent of its mode of formation. (the *Bohr independence hypothesis* or the *amnesia assumption*). While this statement is not true in general, it remains a useful tool for understanding certain features of compound nuclear reactions. For example, let us consider the classical work of Ghoshal (Phys. Rev. **80**, 939 (1950)). Ghoshal formed the compound nucleus ^{64}Zn in two ways, *i.e.*, by bombarding ^{63}Cu with protons and by bombarding ^{60}Ni with alpha particles. He examined the relative amounts of ^{62}Cu , ^{62}Zn and ^{63}Zn found in the two bombardments and within his experimental uncertainty of 10%, he found the amounts of the products were the same in both bombardments. (Later experiments have shown smaller scale deviations from the independence hypothesis).

Because of the long time scale of the reaction and the “amnesia” of the compound nucleus about its mode of formation, one can show that the angular distribution of the products is symmetric about 90 degrees (in the frame of the moving compound nucleus).

The cross section for a compound nuclear reaction can be written as the product of two factors, the probability of forming the compound nucleus and the probability that the compound nucleus decays in a given way. As described above, the probability of forming the compound nucleus can be written as

$$\sigma = \pi \lambda^2 \sum_{\ell=0}^{\infty} (2\ell + 1) \Gamma_{\ell}$$

The probability of decay of the compound nucleus into a given set of products β can be written as

$$probability = \left[\frac{T_\ell^\beta(E_\beta)}{\sum_{\ell_\gamma, E_\gamma} T_\ell^\gamma(E_\gamma)} \right]$$

where T_l is the transmission coefficient for CN decay into products i. Figure 10-16 shows a schematic view of the levels of the compound nucleus.

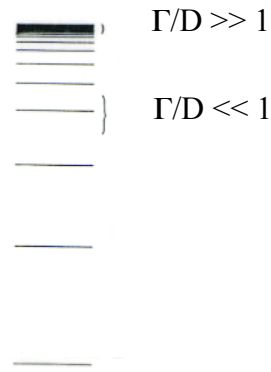


Figure 10-17 Schematic view of the levels of a compound nucleus.

Note the increasing number of levels as the CN excitation energy increases.

Quantitatively, the number of levels per MeV of excitation energy, E , increases approximately exponentially as $E^{1/2}$.

The interesting categories of CN reactions can be defined by the ratio of the width of a compound nucleus level, Γ , to the average spacing between compound nuclear levels, D . (Recall from the Heisenberg uncertainty principle that $\Gamma \cdot \tau \geq \hbar$, where τ is the mean life of a compound nucleus level.) The categories are (a) $\Gamma/D \ll 1$, i.e., the case of isolated non-overlapping levels of the compound nucleus and (b)

$\Gamma/D \gg 1$, the case of many overlapping levels in the compound nucleus. (Figure 10-17). Intuitively category (a) reactions are those in which the excitation energy of the compound nucleus is low while category (b) reactions are those in which the excitation energy is high.

Let us first consider the case of $\Gamma/D \ll 1$. This means that at certain values of the compound nucleus excitation energy, individual levels of the compound nucleus can be excited (*i.e.*, when the excitation energy exactly equals the energy of a given CN level.) When this happens, there will be a sharp rise or *resonance* in the reaction cross section akin to the absorption of infrared radiation by sodium chloride when the radiation frequency equals the natural crystal oscillation frequency. In this case, the formula for the cross section (the *Breit-Wigner single level formula*) for the reaction $a + A \rightarrow C \rightarrow b + B$ is

$$\sigma = \pi D^2 \frac{(2J_C + 1)}{(2J_A + 1)(2J_a + 1)} \frac{\Gamma_{aA} \Gamma_{bB}}{(\varepsilon - \varepsilon_0)^2 + \left(\frac{\Gamma}{2}\right)^2}$$

where J_i is the spin of i^{th} nucleus, Γ_{aA} , Γ_{bB} , and Γ are the partial widths for the formation of C , the decay of C into $b+B$ and the total width for the decay of C , respectively. The symbols ε and ε_0 refer to the energy of the projectile nucleus and the projectile energy corresponding to the excitation of a single isolated level.

Applying this formula to the case of (n,γ) reactions gives

$$\sigma_{n,\gamma} = \pi D^2 \frac{(2J_C + 1)}{(2J_A + 1)(2)} \frac{\Gamma_n \Gamma_\gamma}{(\varepsilon - \varepsilon_0)^2 + \left(\frac{\Gamma}{2}\right)^2}$$

An example of this behavior is shown in Figure 10-18.

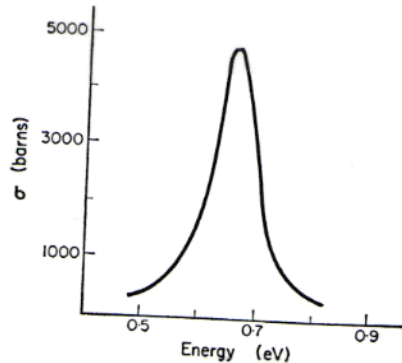


Figure 10-18 Resonance behavior in (n,γ) reactions.

Resonances are seen in low energy neutron induced reactions where one is populating levels in the compound nucleus at excitation energies of the order of the neutron binding energy where the spacing between levels is of the order of eV. For neutron energies well below ε_0 , so that $(\varepsilon - \varepsilon_0)^2 \approx \varepsilon_0^2$, then the cross section for the (n,γ) reaction goes as $1/v$ where v is the neutron velocity, a general behavior described earlier.

Let us now consider the case where $\Gamma/D \gg 1$, i.e., many overlapping levels of the compound nucleus are populated. (We are also tacitly assuming a large range of compound nuclear excitation energies). The cross section for the reaction $a + A \rightarrow C \rightarrow b + B$ can be written as

$$\sigma_{ab} = \sigma_C P_C(b)$$

where $\sigma_C(a)$ is the cross section for the formation of the compound nucleus C and P_C is the probability that C will decay to form $b + B$. Clearly $\sum P_C(b) = 1$. Now let us consider, in detail,

the probability that emitted particle b has an energy ε_b . First of all, we can write down that the maximum energy that b can have is $E_C^* - S_b$ where E_C^* is the excitation energy of the compound nucleus and S_b is the separation energy of b in the residual nucleus B. But b can be emitted with a variety of energies less than this with the result that the nucleus B will be left in an excited state. By using the arguments of detailed balance from statistical mechanics (see Lefort, FKMM) we can write for the probability of emitting a particle b with an energy ε_b ($< \varepsilon_{\max}$, leaving the nucleus B at an excitation energy E_B^*)

$$W_b(\varepsilon_b) d\varepsilon_b = \frac{(2J_b + 1)\mu}{\pi^2 h^3} \varepsilon_b \sigma_{inv} \frac{\rho(E_B^*)}{\rho(E_C^*)} d\varepsilon_b$$

In this equation, μ is the reduced mass of the system and σ_{inv} is the cross section for the inverse process in which the particle b is captured by the nucleus B where b has an energy, ε_b . The symbols $\rho(E_B^*)$ and $\rho(E_C^*)$ refer to the level density in the nucleus B excited to an excitation energy E_B^* and the level density in the compound nucleus C excited to an excitation energy, E_C^* . The inverse cross section can be calculated using the same formulas used to calculate the compound nucleus formation cross section. Using the Fermi gas model, we can calculate the level densities of the excited nucleus as

$$\rho(E^*) = C \exp\{2(aE^*)^{1/2}\}$$

where the *level density parameter*, a , is $A/12 - A/8$. The nuclear temperature T is given by the relation

$$E^* = aT^2 - T$$

The ratio of emission widths for emitted particles x and y is given as

$$\frac{\Gamma_x}{\Gamma_y} = \frac{g_x \mu_x}{g_y \mu_y} \frac{R_x}{R_y} \frac{a_x}{a_y} \exp \left\{ (a_x R_x)^{1/2} - 2(a_y R_y)^{1/2} \right\}$$

where g_i is the spin of the i^{th} particle, a_i and R_i are the level density parameter and maximum excitation energy for the residual nucleus that results from the emission of the i^{th} particle. R is formally $E^* - S - \epsilon_s$ where ϵ_s is the threshold for charged particle emission (ϵ_s for neutrons is 0).

If the emitted particles are neutrons, the emitted neutron energy spectrum has the form

$$N(\varepsilon) d\varepsilon = \frac{\varepsilon}{T^2} \exp(-\varepsilon/T) d\varepsilon$$

as shown in Figure 10-19.

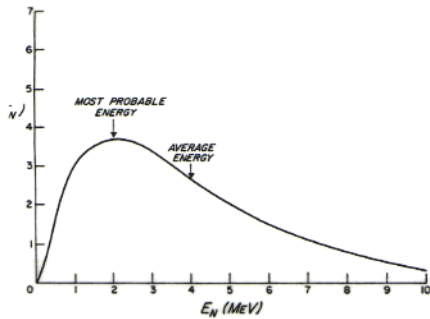


Figure 10-19. Spectrum of evaporated neutrons.

In other words, the particles are emitted with a Maxwellian energy distribution. The most probable energy is T while the average energy is $2T$. What we are saying is that the compound nucleus “evaporates” particles like molecules leaving the surface of a hot liquid. By measuring the energy spectrum of the particles emitted in a compound nuclear reaction, we are using a “nuclear thermometer” in that

$$\frac{\frac{d(\ln N(\varepsilon) d\varepsilon)}{d\varepsilon}}{\frac{\varepsilon \sigma_{inv}}{d\varepsilon}} = \frac{1}{T}$$

Charged particles may also be evaporated except the minimum kinetic energy is not zero as it is for neutrons. Instead the threshold for charged particle emission ε_s (which is approximately the Coulomb barrier) determines the minimum energy of an evaporated particle. (see Figure 10-10). The energy spectrum of evaporated charged particles is

$$N(\varepsilon) d\varepsilon = \frac{\varepsilon - \varepsilon_s}{T^2} \exp(-(\varepsilon - \varepsilon_s)/T) d\varepsilon$$

What will be the distribution in space of the reaction products? Let us assume that because the compound nucleus has “forgotten” its mode of formation, there should be no preferential direction for the emission of the decay products. Thus we might expect that all angles of emission of the particles, θ , to be equally probable. Thus we would expect that $P(\theta)$, the probability of emitting a particle at an angle θ , might be a constant. Then we would expect that $d\sigma/d\Omega(\theta)$ would be given as

$$\frac{d\sigma}{d\Omega}(\theta) = P(\theta) \frac{d\theta}{d\Omega}$$

This assumes that we are making the measurement of the emitted particle angular distribution in the frame of the moving compound nucleus. In the laboratory frame, there will appear to be more particles emitted in the forward direction (with higher energies) than are emitted in the backward direction)

The energy variation of the cross section (the *excitation function*) for processes involving evaporation is fairly distinctive as shown in Figure 10-20, where the excitation function for the $^{209}\text{Bi}(\alpha, \text{xn})$ reaction is shown. Starting from the threshold ε_s , the cross section rises with increasing energy because the formation cross section for the compound nucleus is increasing. Eventually the excitation energy of the compound nucleus becomes large enough that emission of two neutrons is energetically possible. This “2n out” process will dominate over the “1n out”

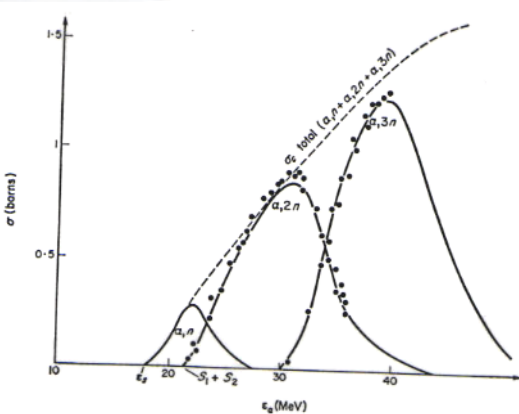


Figure 10-20 Excitation function the for $^{209}\text{Bi}(\alpha, \text{xn})$ reaction.

process and the cross section for the “1n out” process will decrease. Eventually the “3n out” process will dominate over the “2n out” process. We expect the peaks for the individual “xn out” processes to be at $S_{n1} + 2T$, $S_{n1} + S_{n2} + 4T$, $S_{n1} + S_{n2} + S_{n3} + 6T$, etc. (where we neglect any changes in T during the emission process)

Let us recapitulate what we have said about compound nuclear reactions. We have said that they are basically nuclear reactions with a long-lived reaction

intermediate, which is formed by a complicated set of two-body interactions. We can write down a set of equations that describes the overall compound nuclear cross section. We have shown how this general formula simplifies for specific cases, the case of exciting a single level of the compound nucleus where we see spikes or resonances in the cross section and the case of higher excitation energies where the compound nucleus behaves like a hot liquid, evaporating particles. At all excitation energies, the angular distribution of the reaction products is symmetric with respect to a plane perpendicular to the incident particle direction.

10.10 Photonuclear Reactions

Photonuclear reactions are nuclear reactions in which the incident projectile is a photon and the emitted particles are either charged particles or neutrons. Examples of such reactions are reactions like (γ, p) , (γ, n) , (γ, α) , etc. The high energy photons needed to induce these reactions can be furnished from the annihilation of positrons in flight (producing monoenergetic photons) or the energetic bremsstrahlung from slowing down high energy electrons (producing a continuous distribution of photon energies). A special feature of the excitation function for photonuclear reactions is the appearance of a large bump in the cross section at ~ 25 MeV for reaction with a ^{16}O target that slowly changes with A until it is at ~ 15 MeV for ^{208}Pb . (Figure 10-21)

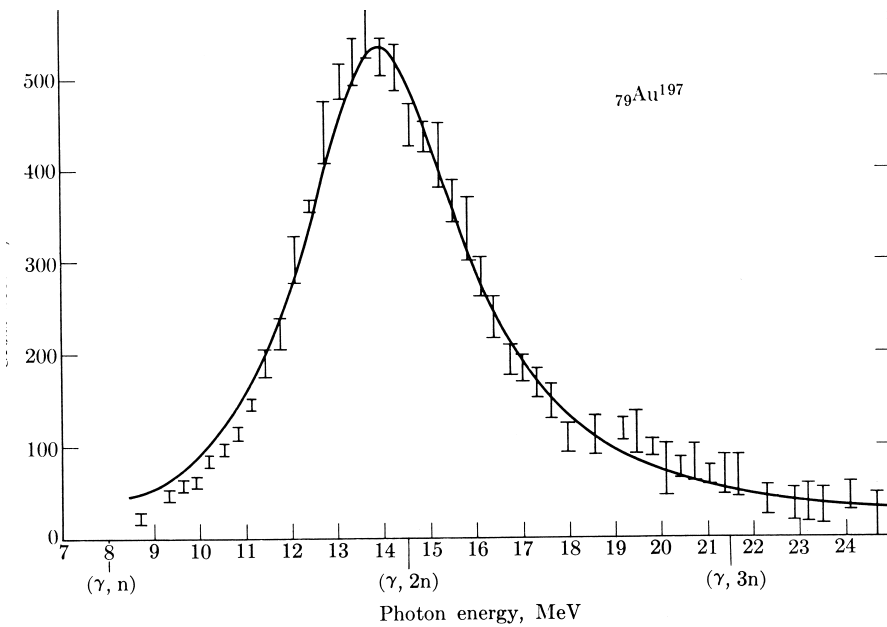


Figure 10-21. The photonuclear cross section of ^{197}Au . From Fultz, et al., Phys. Rev.

127, 1273 (1962).

This bump is called the *giant dipole resonance*. Goldhaber and Teller provided a model for this reaction in which the giant dipole resonance is due to a huge collective vibration of all the neutrons versus all the protons. This model suggests the energy of the GDR should vary as $A^{-1/6}$, in fair agreement with observations. In deformed nuclei, the GDR is split into two components, representing oscillations along the major and minor nuclear axes. One further fact about photonuclear reactions should be noted. The sum of the absorption cross section for dipole photons (over all energies) equals some constant, *i.e.*,

$$\int_0^{\infty} \sigma_{abs}(E_{\gamma}) dE_{\gamma} \propto \frac{NZ}{A} \approx 0.058 \frac{NZ}{A} \text{ MeV - barns}$$

This is called the *dipole-sum rule*

10.11 Heavy Ion Reactions.

Heavy ion induced reactions are usually taken as reactions induced by projectiles heavier than an alpha particle. The span of projectiles studied is large, ranging from the light ions, C, O, Ne to the medium mass ions, such as S, Ar, Ca, Kr to the heavy projectiles, Xe, Au and even U. Reactions induced by heavy ions have certain unique characteristics that distinguish them from other reactions. The wave length of a heavy ion at an energy of 5 MeV/ nucleon or more is small compared to the dimensions of the ion. As a result, the interactions of these ions can be described classically. The value of the angular momentum in these collisions is relatively large. For example we can write

$$\ell_{\max} = \frac{R}{\lambda} \left(1 - \frac{B}{E}\right)^{1/2}$$

For the reaction of 226 MeV ^{40}Ar + ^{165}Ho , we calculate $\ell_{\max} = 163^\circ$. This is relatively large compared to the angular momenta involved in nucleon-induced reactions. Lastly, quite often the product of the atomic numbers of the projectile and target is quite large (> 1000), indicating the presence of large Coulomb forces acting in these collisions.

The study of heavy ion-induced reactions is a forefront area of nuclear research. By using heavy ion-induced reactions to make unusual nuclear species, one can explore various aspects of nuclear structure and dynamics "at its limits" and thus gain a deeper insight. Another major thrust is to study the dynamics and thermodynamics of the colliding nuclei.

In Figure 10-22, we show a cartoon of the various impact parameters and trajectories one might see in a heavy ion reaction.

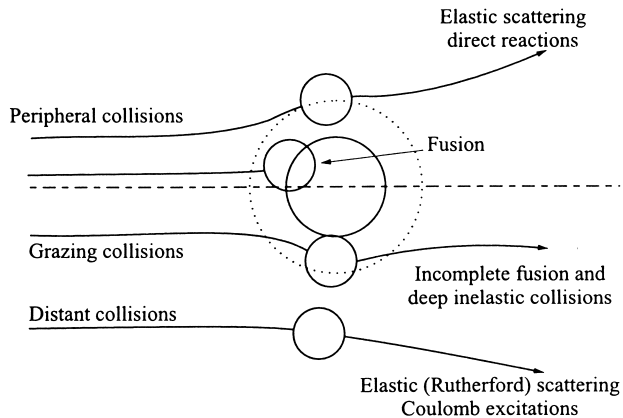


Figure 10-22. Classification scheme of collisions based upon impact parameter. From Gladioli.

The most distant collisions lead to elastic scattering and Coulomb excitation. Coulomb excitation is the transfer of energy to the target nucleus via the long range Coulomb interaction to excite the levels of the target nucleus. Grazing collisions lead to inelastic scattering and the onset of nucleon exchange. Head-on or near head-on collisions lead to fusion of the reacting nuclei which can lead to the formation of a compound nucleus or a "quasi-fusion" reaction in which there is substantial mass and energy exchange between the projectile and target nuclei without the "true amnesia" characteristic of compound nucleus formation. For impact parameters between the grazing and head-on collisions, one observes a new type of nuclear reaction mechanism, *deep inelastic scattering*. In deep inelastic

scattering, the colliding nuclei touch, partially amalgamate, exchange substantial amounts of energy and mass, rotate as a partially fused complex, and then reseparate under the influence of their mutual Coulomb repulsion.

The same range of reaction mechanisms can be depicted in terms of the angular momentum transfer associated with each of the mechanisms. (Figure 10-23).

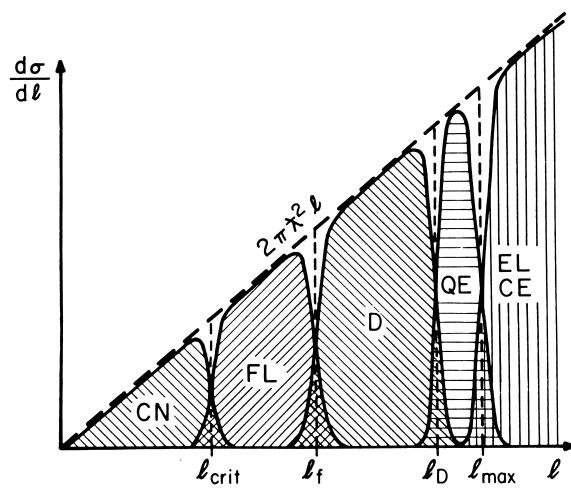


Figure 10-23. Schematic illustration of the ℓ dependence of the partial cross section for compound nucleus (CN), fusion-like (FL), deep inelastic (D), quasielastic (QE), Coulomb excitation (CE), and elastic (EL) processes. From Schroeder and Huizenga in *Treatise on Heavy Ion Science, Volume 2* (Plenum, New York, 1984), D.A. Bromley, ed., p 242.

The most peripheral collisions lead to elastic scattering and thus the highest values of the angular momentum transfer, ℓ . The grazing collisions lead to inelastic scattering and nucleon exchange reactions, which are lumped together as

"quasielastic" reactions. Solid-contact collisions lead to deep inelastic collisions, corresponding to intermediate values of ℓ . The most head-on collisions correspond to compound nucleus formation and thus the lowest values of the angular momentum transfer, ℓ . Slightly more peripheral collisions lead to the fusion-like or quasifusion reactions.

10.11.1 Coulomb Excitation

The potential energy due to the Coulomb interaction between a heavy ion and a nucleus can be written as

$$E_c = (Z_1 Z_2 e^2 / R) \sim 1.2 (Z_1 Z_2 / A^{1/3}) \text{ MeV}$$

Because of the strong, long-range electric field between projectile and target nuclei, it is possible for the incident heavy ion to excite the target nucleus electromagnetically. This is called *Coulomb excitation* or *Coulex*. Rotational bands in deformed target nuclei may be excited by the absorption of dipole photons. This technique is useful for studying the structure of such nuclei. Since the cross sections for these reactions are very large (involving long range interactions with the nucleus) they are especially suitable for use when studying the structure of exotic nuclei with radioactive beams where the intensities are low (Glasmacher). At relativistic energies, the strong electric field of the incident ion may be used to disintegrate the target nucleus (*electromagnetic dissociation*).

10.11.2 Elastic Scattering

In Figure 10-23, we compare elastic scattering for the collision of light nuclei with that observed in collisions involving much heavier nuclei. Collisions between the light nuclei show the characteristic Fraunhofer diffraction pattern discussed

earlier, in connection with the scattering of nucleons. The large Coulomb force associated with the heavier nucleus acts as a

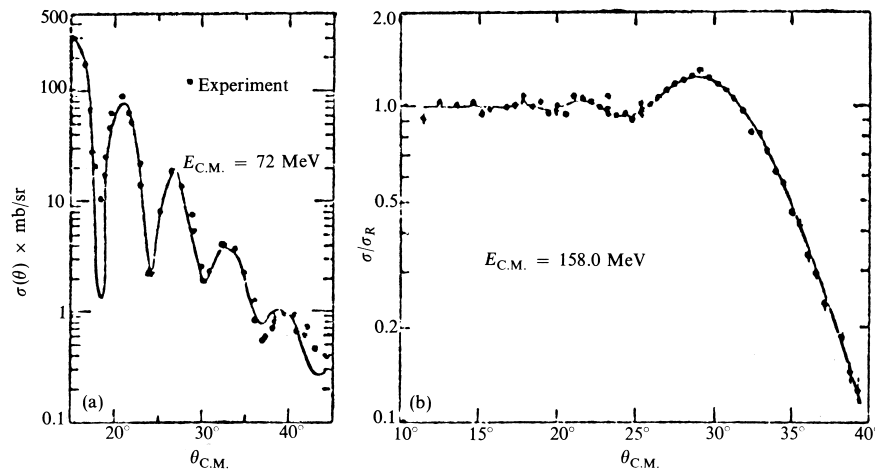


Figure 10-24. Angular distribution for $^{12}\text{C} + ^{16}\text{O}$ elastic scattering, showing Fraunhofer diffraction and the elastic scattering of ^{16}O with ^{208}Pb which shows Fresnel diffraction. From Valentin.

diverging lens causing the diffraction pattern to be that of Fresnel diffraction. For the case of Fresnel diffraction, special emphasis is given to the point in the angular distribution of the scattered particle where the cross section is $1/4$ that of the Rutherford scattering cross section. This "quarter-point angle" corresponds to the classical grazing angle. Note that the elastic scattering cross section equals the Rutherford scattering cross section at scattering angles significantly less than the "quarter point" angle. Since the Rutherford scattering cross section is calculable, this fact allows experimentalists to measure the number of elastically scattered

particles at angles less than the quarter point angle to deduce/monitor the beam intensity in heavy ion induced reaction studies.

10.11.3 Fusion Reactions

In Figure 10-25, we show another representation of the difference between the various reaction mechanisms in terms of the energy needed to induce the reactions.

We have the energy needed to bring the ions in contact and thus interact, the *interaction barrier*, $V(R_{int})$. Formally Bass has shown the reaction cross section can be expressed in terms of this interaction barrier as

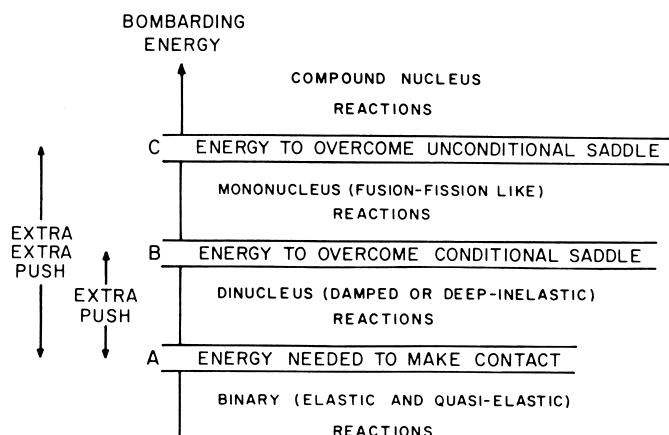


Figure 10-25. Schematic illustration of the three critical energies and the four types of heavy ion nuclear reactions. From Schroeder and Huizenga in *Treatise on Heavy Ion Science, Volume 2* (Plenum, New York, 1984), D.A. Bromley, ed., p 679

$$\sigma_R = \pi R_{\text{int}}^2 \left[1 - \frac{V(R_{\text{int}})}{E_{cm}} \right]$$

where the interaction radius is given as

$$R_{\text{int}} = R_1 + R_2 + 3.2 \text{ fm}$$

where the radius of the i^{th} nucleus is

$$R_i = 1.12 A_i^{1/3} - 0.94 A_i^{-1/3} \text{ fm}$$

and the interaction barrier is given as

$$V(R_{\text{int}}) = 1.44 \frac{Z_1 Z_2}{R_{\text{int}}} - b \frac{R_1 R_2}{R_1 + R_2}$$

where $b \sim 1 \text{ MeV/fm}$. The energy necessary to cause the ions to interpenetrate to cause quasifusion is called the *extra push energy*. The energy necessary to cause the ions to truly fuse and forget their mode of formation is referred to as the *extra-extra push energy*.

The probability of fusion is a sensitive function of the product of the atomic numbers of the colliding ions. The abrupt decline of the fusion cross section as the Coulomb force between the ions increases is due to the emergence of the deep inelastic reaction mechanism. This and other features of the fusion cross section can be explained in terms of the potential between the colliding ions. This potential consists of three contributions, the Coulomb potential, the nuclear potential and the centrifugal potential. The variation of this potential as a function of the angular momentum ℓ is shown as Figure 10-26.

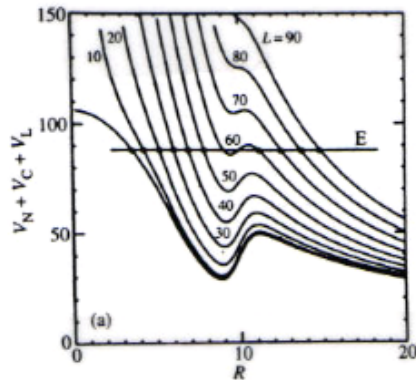


Figure 10-26. Sum of the nuclear, Coulomb and centrifugal potential for $^{18}\text{O} + ^{120}\text{Sn}$ as a function of radial distance for various values of the orbital angular momentum

ℓ .

Note that at small values of the angular momentum, there is a pocket in the potential. Fusion occurs when the ions get trapped in this pocket. If they do not get trapped they do not fuse. With high values of the Coulomb potential, there are few or no pockets in the potential for any value of ℓ , thus no fusion occurs. For a given projectile energy and Coulomb potential, there is a value of the angular momentum above which there are no pockets in the potential (the critical value of the angular momentum) and thus no fusion occurs.

As shown in Figure 10-26, there is an ℓ -dependent barrier to fusion that is the sum of the nuclear, Coulomb and centrifugal potentials. This barrier is also a sensitive function of the relative deformation and orientation of the colliding ions. In Figure 10-27, we show the excitation function for fusion of ^{16}O with various isotopes of Sm.

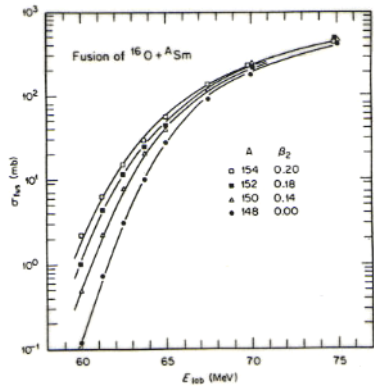


Figure 10-27. Fusion cross sections for $^{16}\text{O} + {}^A\text{Sm}$.

One observes a significantly lower threshold and enhanced cross section for the case where the ^{16}O ion interacts with deformed ^{154}Sm compared to near-spherical ^{148}Sm . This enhancement is the result of the lowering of the fusion barrier for the collision with the deformed nucleus due to the fact that the ions will contact at a larger value of R resulting in a lower Coulomb component of the potential. Let us now consider what happens after the formation of a compound nucleus in a heavy ion fusion reaction. In Figure 10-28, we show the predictions for the decay of the compound nuclei formed in the reaction of 147 MeV ${}^{40}\text{Ar}$ with ${}^{124}\text{Sn}$ to form ${}^{164}\text{Er}$ at an excitation energy of 53.8 MeV. The angular momentum distribution in the compound nucleus shows population of states with $\ell = 0 - 60 \hbar$. The excitation energy is such that energetically the

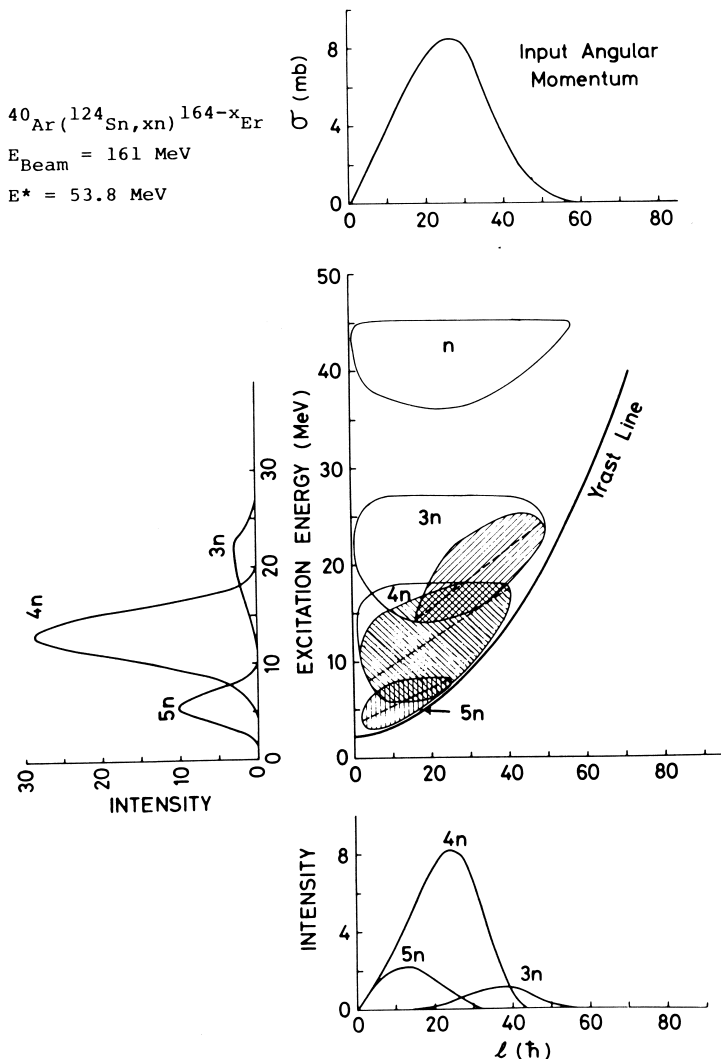


Figure 10-28. Predicted decay of the ${}^{164}\text{Er}$ compound nuclei formed in the reaction of ${}^{40}\text{Ar}$ with ${}^{124}\text{Sn}$. [From Stokstad (1985).]

preferred reaction channel involves the evaporation of 4 neutrons from the compound nucleus. As the compound nucleus evaporates neutrons the angular momentum does not change dramatically since each neutron removes a relatively small amount of angular momentum. Eventually the yrast line restricts the population of states in the E-J plane. The yrast line is the locus of the lowest lying

state of a given angular momentum for a given J value. Below the yrast line for a given J, there are not states of the nucleus. (The word yrast is from the Old Norse for the "dizziest"). When the system reaches the yrast line, it decays by a cascade of gamma rays. Heavy ion reactions are thus a tool to excite levels of the highest spin in nuclei allowing the study of nuclear structure at high angular momentum.

10.11.4 Deep Inelastic Scattering

Now let us turn our attention to the case of deep inelastic scattering. In the early 1970s, as part of a quest to form superheavy elements by the fusion of Ar and Kr ions with heavy target nuclei, one discovered a new nuclear reaction mechanism, deep inelastic scattering. For example, in the reaction of ^{84}Kr with ^{209}Bi , (Figure 10-29) instead of observing the fission of the completely fused nuclei (to form nuclei in the region denoted by the triangle), one observed projectile and target like nuclei and a new and unexpected group of fragments with masses near that of the target and projectile but with kinetic energies that were much lower than those expected from elastic or quasielastic scattering.

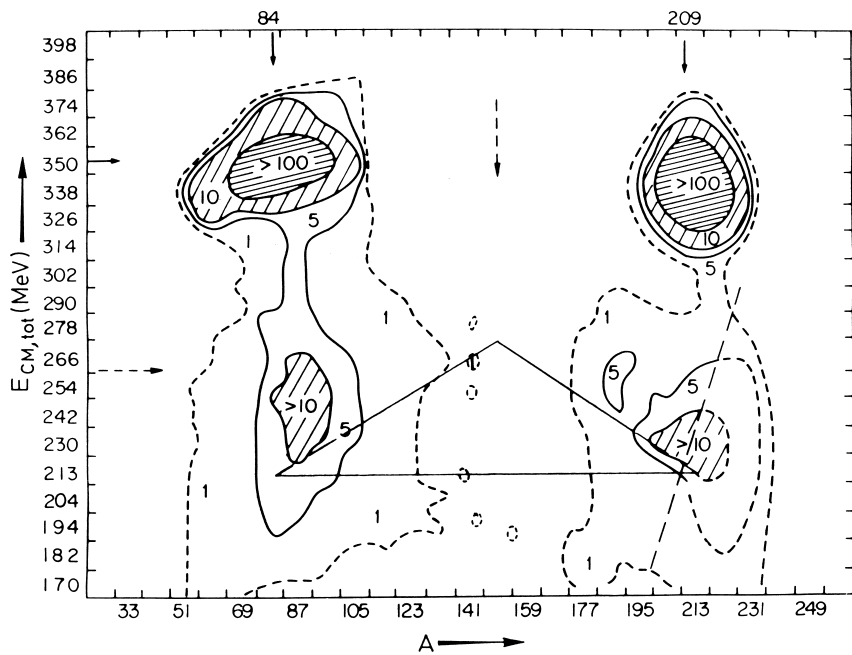


Figure 10-29. Measurement of the product energy and mass distributions in the reaction of ^{84}Kr with ^{209}Bi . [From M. Lefort et al., Nucl. Phys. A216, 166 (1973)]

These nuclei appeared to be nuclei that had undergone an inelastic scattering that had resulted in the loss of a large amount of the incident projectile kinetic energy. Further measurement revealed this to be a general phenomenon in reactions where the product of the atomic numbers of the colliding ions was large. (>2000). As described earlier, the ions come together, interpenetrate partially, exchange mass, energy and charge in a diffusion process and then reseparate under the influence of their mutual Coulomb repulsion. The initial projectile energy is damped into the excitation energy of the projectile and target-like fragments. As a consequence, the larger the kinetic energy loss, the broader the distribution of the final products becomes.

10.11.5 Incomplete Fusion

In the course of the fusion of the projectile and target nuclei, it is possible that one of them will emit a single nucleon or a nucleonic cluster prior to the formation of a completely fused system. Such processes are referred to as *pre-equilibrium emission* (in the case of nucleon emission) or *incomplete fusion* (in the case of cluster emission). As the projectile energy increases, these processes become more important and they generally dominate over fusion at projectile energies above 20 MeV/nucleon. As a consequence of these processes, the resulting product nucleus has a momentum that is reduced relative to complete fusion events. Measurement of the momentum transfer in the collision serves as a measure of the occurrence of these phenomena. In the spectra of emitted particles, a high-energy tail on the normal evaporation spectrum is another signature of pre-equilibrium emission.

10.11.6 Reactions Induced by Radioactive Projectiles

There are a few hundred stable nuclei but several thousand nuclei that are radioactive and have experimentally useful lifetimes. In the past decade, one of the fastest growing areas of research in nuclear science has been the study of nuclear reactions induced by radioactive projectiles. Using either ISOL or PF techniques, several hundred new radioactive nuclear beams have become available (see Chapter 14).

The principal attraction in these studies is the ability to form reaction products or reaction intermediates with unusual N/Z ratios. By starting with reacting nuclei that are either very proton-rich or very neutron-rich, new regions of

nuclei can be reached and their properties studied. At higher energies, the isospin of the intermediate species may be unusual, allowing one to determine the effect of isospin on the properties of highly excited nuclear matter. Occasionally the radioactive beams themselves have unusual structure, *i.e.*, ^{11}Li , and their properties and reactions are of interest.

10.12 High Energy Nuclear Reactions

A nuclear reaction is said to be a *low energy reaction* if the projectile energy is ≤ 10 MeV/nucleon. A nuclear reaction is termed a *high-energy reaction* if the projectile energy is ≥ 400 MeV/nucleon. (Not surprisingly the reactions induced by 20-250 MeV/nucleon projectiles are called *intermediate energy reactions*.)

What distinguishes low and high-energy reactions? In low energy nuclear collisions, the nucleons of the projectile interact with the average or mean nuclear force field associated with the entire target nucleus. In a high-energy reaction, the nucleons of the projectile interact with the nucleons of the target nucleus individually, as nucleon-nucleon collisions. To see why this might occur, let us compute the de Broglie wave length of a 10 MeV proton and a 1000 MeV proton. We get $\lambda_{10\text{ MeV}} = 9.0$ fm and $\lambda_{1000\text{ MeV}} = 0.73$ fm. The average spacing between nucleons in a nucleus is ~ 1.2 fm. Thus we conclude that at low energies, the projectile nucleons can interact with several nucleons at once while at high energies, collisions occur between pairs of nucleons.

10.12.1 Spallation/Fragmentation

What type of reactions do we observe at high energies? Because we are dealing with nucleon-nucleon collisions, we do not expect any significant amount of compound nucleus formation. Instead most reactions should be direct reactions taking place on a short time scale. In Figure 10-30, we show a typical distribution of the masses of the residual nuclei from the interaction of GeV protons with a heavy nucleus, like ^{209}Bi .

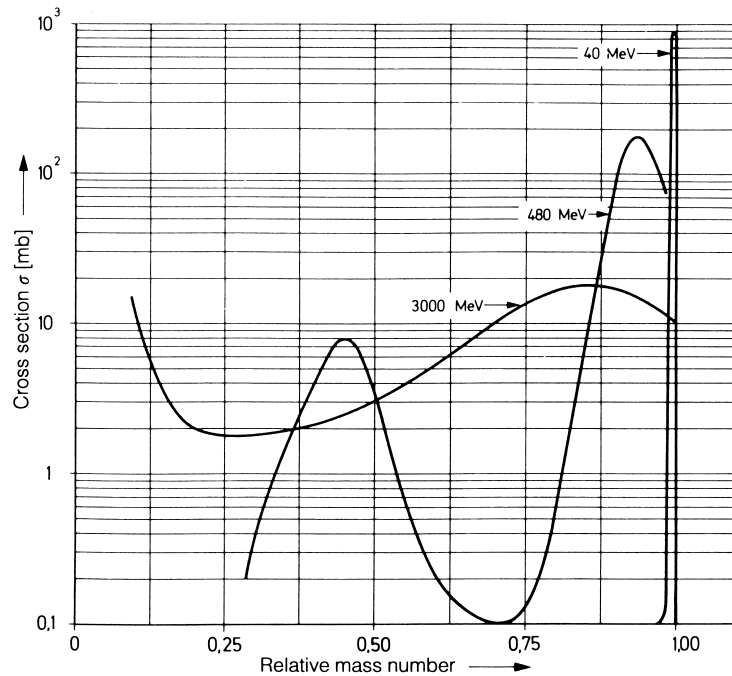


Figure 10-30. Mass distribution for $p + ^{209}\text{Bi}$. From Miller and Hudis, Ann. Rev. Nucl. Sci. **9**, 159 (1959).

One observes a continuous distribution of product masses ranging from the target mass to very low values of A. Three regions can be identified in the yield distributions. One region is centered around $A_{\text{target}}/2$ ($A=50-140$) and consists of

the products of the fission of a target-like nucleus. For larger A values ($A_{\text{fragment}} \geq (2/3) A_{\text{target}}$) the products are thought to arise from a direct reaction process termed *spallation*. The incident proton knocks out several nucleons in a series of two-body collisions, leaving behind a highly excited heavy nucleus. This nucleus decays by the evaporation of charged particles and neutrons, forming a continuous distribution of products ranging downward in A from the target mass number. The term spallation was given to this phenomenon by one of us (GTS) after consultation with a professor of English who assured him that the verb "to spall" was a very appropriate term for this phenomenon. For the lowest mass numbers ($A_{\text{fragment}} \leq (1/3) A_{\text{target}}$) one observes another group of fragments that are termed to be *intermediate mass fragments*. These fragments are thought to arise from the very highly excited remnants of the most head-on collisions by either sequential particle emission or a nuclear shattering or multifragmentation process.

The course of a reaction at high energies is different than one occurring at lower energies. As mentioned earlier, collisions occur between pairs of nucleons rather than having one nucleon collide with several nucleons simultaneously. The cross section for nucleon-nucleon scattering varies inversely with projectile energy. At the highest energies, this cross section may become so small that some nucleons will pass through the nucleus without undergoing any collisions, *i.e.*, the nucleus appears to be *transparent*.

In this regard, a useful quantitative measure of the number of collisions a nucleon undergoes in traversing the nucleus is the *mean free path*, Λ . Formally we have

$$\Lambda = 1/\rho\sigma$$

where σ is the average nucleon-nucleon scattering cross section ($\sim 30 \text{ mb}$) and ρ is the nuclear density ($\sim 10^{38} \text{ nucleons/cm}^3$). Thus the mean free path is $\sim 3 \times 10^{-13} \text{ cm}$. In each collision, the kinetic energy imparted to the struck nucleon is $\sim 25 \text{ MeV}$ and thus the struck nucleon may collide with other nucleons, generating a *cascade* of struck particles. (see Figure 10-31).

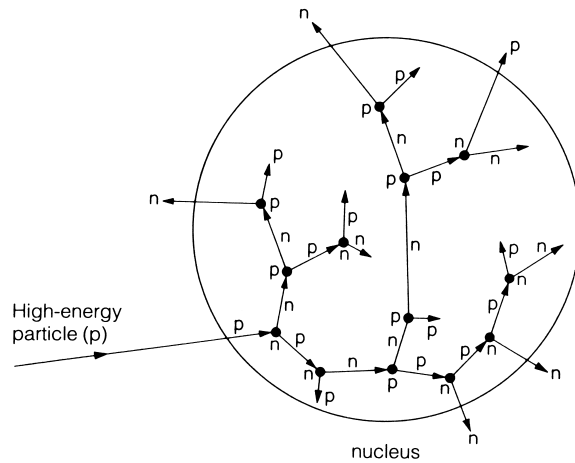


Figure 10-31. Schematic view of nuclear cascade. [From Lieser (1997)].

If the energy of the incident nucleon exceeds $\sim 300 \text{ MeV}$, then it is possible to generate π mesons in these collisions, which, in turn, can interact with other nucleons. A typical time scale for the cascade is 10^{-22} sec . The result of this *intranuclear cascade* is an excited nucleus, which may decay by pre-equilibrium emission of particles, evaporation of nucleons, sequential emission of IMFs or disintegration into multiple fragments.

In the mid-1970s, at the Bevalac in Berkeley, one initiated the study of heavy ion reactions at very high energies (0.250 - 2.1 GeV/nucleon). At these high projectile energies, a number of observations were interpreted in terms of a simple geometric model referred to as the abrasion-ablation or fireball model. (Figure 10-32) In this model the incoming projectile

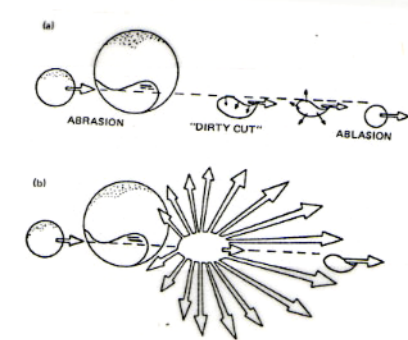


Figure 10-32 The abrasion -ablation model of relativistic nuclear collisions.

sheared off a sector of the target (corresponding to the overlap region of the projectile and target nucleus--the "abrasion' step). The non-overlapping regions of the target and projectile nuclei were assumed to be left essentially undisturbed and unheated, the so-called "spectators" to the collision. The hot overlap region (the "participants") formed a "fireball" that decayed with the release of nucleons and fragments. The wounded target nucleus was expected to have a region of extra surface area exposed by the projectile cut through it. Associated with this extra surface area is an excitation energy corresponding to the surface area term of the semi-empirical mass equation of about 1 MeV per excess fm² of surface area. As the

nucleus relaxes, this excess surface energy becomes available as excitation energy and results in the normal emission of nucleons and fragments (the "ablation" step).

The use of this simple model for high energy nucleus-nucleus collisions has resulted in a general categorization of energetic nucleus-nucleus collisions as either "peripheral" or "central". In peripheral reactions, one has large impact parameters and small momentum transfer. Such reactions, which produce surviving large spectators, are referred to as *fragmentation* reactions. Such reactions are of interest in the production of new radioactive nuclei and radioactive beams.

10.12.2 Multifragmentation

In central collisions one has smaller impact parameters and larger energy and momentum transfer. In central nucleus-nucleus collisions at intermediate energies (20 – 200 MeV/nucleon), large values of the nuclear excitation energy (>1000 MeV) and temperature (> 10 MeV) may be achieved for short periods of time (10^{-22} sec). Nuclei at these high excitation energies can decay by the emission of complex or intermediate mass fragments (IMFs). (An IMF is defined as a reaction product whose mass is greater than 4 and less than that of a fission fragment).

Multifragmentation occurs when several IMFs are produced in a reaction. This can be the result of sequential binary processes, "statistical" decay into many fragments (described by passage through a transition state or the establishment of statistical equilibrium among fragments in a critical volume), or a dynamical process in which the system evolves into regions of volume and surface instabilities leading to multifragment production.

To investigate these phenomena, it is necessary to measure as many of the emitted fragments and particles from a reaction. As a result, various multidetector arrays have been constructed and used. Quite often these arrays consist of several hundred individual detectors to detect the emitted IMFs, light charged particles, neutrons, target fragments, etc. As a consequence of the high granularity of these detectors, the analysis of the experimental data is time consuming and difficult. Nonetheless, several interesting developments have occurred in recent years.

One theory to describe multifragmentation postulates the formation of a hot nuclear vapor during the reaction, which subsequently condenses into droplets of liquid (IMFs) somewhere near the critical temperature. First postulated to occur in the interaction of GeV protons with Xe, recent experiments with heavy ions have resulted in deduced temperatures and excitation energies (Fig. 10-33) that resemble calculations for a liquid-gas phase transition.

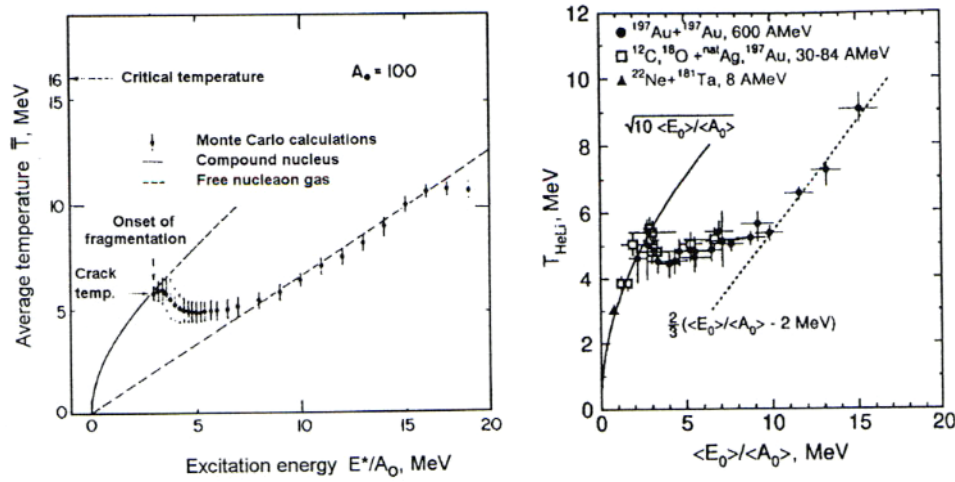


Figure 10-33 Caloric curve as calculated by a multifragmentation model and as measured.

This "caloric curve" shows an initial rise in temperature with excitation energy typical of heating a liquid, followed by a flat region (the phase transition), followed by a region corresponding to heating a vapor.

Finally, there has been an extended debate and discussion of the relative role of statistical and dynamical factors in multifragmentation. The debate has focussed on the observation that the data from several reactions could be plotted such that the probability of emitting multiple fragments, p , could be expressed in a form, $p \exp(-B/T)$, suggestive of the dependence of the fragment emission probabilities upon a single fragment emission barrier, B , a feature suggesting the importance of statistical factors. Others have criticized this observation. The criticisms have focussed on the details of the correlation and evidence for dynamic effects.

10.12.3 The Quark-Gluon Plasma

The primary thrust of studies of central collisions at ultra-relativistic energies (> 5 GeV/nucleon) is to create and observe a new form of matter, the quark-gluon plasma (QGP). The modern theory of the strong interaction, quantum chromodynamics, predicts that while quarks and gluons will be confined within a nucleonic "bag" under normal conditions, deconfinement will occur at sufficiently high energies and densities.

This phase transition (from normal nuclear matter to the QGP) is predicted to occur at energy densities of $1-3$ GeV/fm 3 which can be achieved in collisions at c.m. energies of 17 GeV/nucleon.

The experimental signatures of a phase transition include: (a) suppression of production of the heavy vector mesons J/Ψ and Ψ' and the upsilon states, (b) the creation of a large number of ss quark-antiquark pairs and (c) the momentum spectra, abundance and direction of emission of di-lepton pairs. The first phase experiments in this field have been carried out. Energy densities of ~ 2 GeV/fm³ were created. Strong J/Ψ suppression has been observed relative to p-A collisions along with an increase in strangeness production.

References

Most textbooks on nuclear physics and chemistry have chapters on nuclear reactions. Among the favorites of the authors are the following:

1. W.D. Ehmann and D.E. Vance, *Radiochemistry and Nuclear Methods of Analysis* (Wiley, New York, 1991).
2. P.E. Hodgson, E. Gladioli, and E. Gladioli-Erba, *Introductory Nuclear Physics*, (Clarendon, Oxford, 1997).
3. M. Lefort, *Nuclear Chemistry*, (Van Nostrand, Princeton, 1968).
4. K.S. Krane, *Introductory Nuclear Physics* (Wiley, New York, 1988).
5. K.H. Lieser, *Nuclear and Radiochemistry*, (VCH, Wertheim, 1997).
6. N.A. Jelley, *Fundamentals of Nuclear Physics*, (Cambridge, Cambridge, 1990).
7. J.S. Lilley, *Nuclear Physics* (Wiley, Chichester, 2001).
8. W.E. Meyerhof, *Elements of Nuclear Physics*, (McGraw-Hill, New York, 1967).
9. L. Valentin, *Subatomic physics: nuclei and particles, Volume II*, (North-Holland, Amsterdam, 1981).
10. S.S.M. Wong, *Nuclear Physics, 2nd Edition*, (Wiley, New York, 1998).

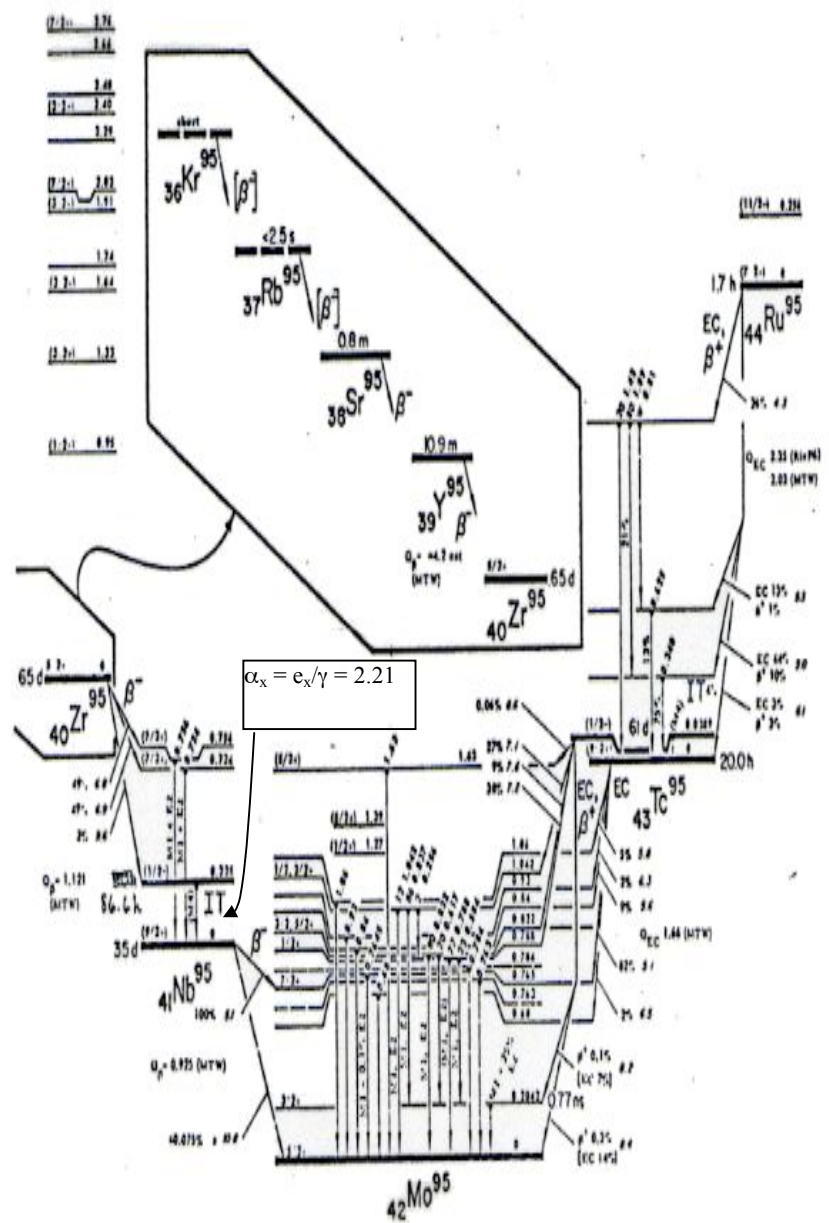
Some specialized references to nuclear reactions that are specially recommended include:

11. R. Bass, *Nuclear Reactions with Heavy Ions* (Springer-Verlag, Berlin, 1980).
12. Nuclides and Isotopes, 15th Edition (General Electric, 1996).
13. G.R. Satchler, *Introduction of Nuclear Reactions, 2nd Edition* (Oxford. New York, 1990).
14. R. Stokstad in *Treatise on Heavy Ion Science, Volume3*, D.A. Bromley, ed. (Plenum, New York, 1985).

Problems

1. Consider the reaction of ^{16}O with ^{64}Ni at a c.m. energy of 48 MeV. What is the lab kinetic energy of the ^{16}O ? What is the Coulomb barrier for the reaction? What is the total reaction cross section? What is the maximum angular momentum brought in by the ^{16}O projectile?
2. One reaction proposed for the synthesis of element 110 is the reaction of ^{59}Co with ^{209}Bi at a laboratory energy of 295 MeV. Calculate the expected total reaction cross section.

3. Define or describe the following terms or phenomena: direct reaction, compound nucleus, stripping reaction.
4. A piece of Au that is 1 mm thick is bombarded for 15 hours by a slow neutron beam of intensity $10^6/\text{sec}$. How many disintegrations per sec of ^{198}Au are present in the sample 24 hours after the end of the bombardment? $\sigma(n,\gamma) = 98.8 \text{ b}$, $t_{1/2}(^{198}\text{Au}) = 2.7 \text{ days}$.
5. What was the rate of production, in atoms per second, of ^{128}I during a constant 1 hour cyclotron (neutron) irradiation of an iodine sample if the sample was found to contain 2.00 mCi of ^{128}I activity at 15 min after end of the irradiation?
6. What is the excitation energy of the ^{116}Sb compound nuclei formed by the bombardment of ^{103}Rh with 50 MeV ^{13}C ions?
7. Neutrons evaporated from a compound nucleus have an average kinetic energy of $\sim 2T$, where T is the nuclear temperature of the residual nucleus. What is the optimum bombarding energy for the production of ^{66}Ga via the $^{65}\text{Cu}(\alpha, 3n)$ reaction if the average nuclear temperature is 1.6 MeV?
8. A 100 mg/cm² thick natural Zr target was bombarded with a beam of 11 MeV protons for one hour (beam current = $25\mu\text{A}$). The $^{95}\text{Nb}^m$ from the reaction $^{96}\text{Zr}(p, 2n)$ was isolated chemically (100% yield) and the k-x-rays resulting from the internal conversion decay of $^{95}\text{Nb}^m$ were counted. In a two hour count beginning 20 hours after the end of bombardment, 1000 counts were observed in the Nb K.-x-ray peak. Given the ^{95}Nb decay scheme shown below and the data given below, calculate the cross section for the $^{95}\text{Zr}(p, 2n) ^{95}\text{Nb}^m$ reaction.
Fluorescence yield = 0.7, efficiency of detection of the K-x-ray is 10^{-3} , $\alpha_k = 2.21$.



9. What is the number of ^{60}Co atoms produced in a 10 mg sample of cobalt metal exposed for 2 minutes to a thermal neutron flux of $2 \times 10^{13} \text{ n/cm}^2\text{sec}$ in a reactor? The cross section for producing $10.5 \text{ min } ^{60}\text{Co}^m$ is 16 barns, while the

cross section for producing 5.3 y ^{60}Co is 20 barns. What is the disintegration rate of the cobalt sample 4 hours after the end of the irradiation?

10. Consider the $^{48}\text{Ca} + ^{248}\text{Cm}$ reaction where the lab energy of the ^{48}Ca is 300 MeV. What is the excitation energy of the putative compound nucleus $^{296}116$? What is the expected total reaction cross section?

11. Consider the reaction of 30 MeV/nucleon ^{129}Xe with ^{238}U . What is the energy of the elastically scattered ^{129}Xe detected at 10° in the lab system?

12. Consider the $^{40}\text{Ca}(\text{d}, \text{p})$ reaction. What would be the most probable angle to detect the protons leading to the first excited state ($3/2^-$) of ^{41}Ca ? What would be their energy if the energy of the incident deuteron beam was 21.0 MeV?

13. Consider you want to make ^{18}F for use in PET studies. What would be the maximum specific activity (dpm/g F) of the ^{18}F made by irradiating 1.0 g of KF in a flux of 10^{10} fast neutrons/cm²-sec. You may assume the $^{19}\text{F}(\text{n}, 2\text{n})$ cross section is 300 mb. Consider you want to produce the ^{18}F carrier free (*i.e.*, with no stable fluorine present). Devise a synthetic scheme for producing the carrier free ^{18}F . Defend your choice of reactions.

14. Consider the nuclide $^{99}\text{Tc}^m$ that is the daughter of ^{99}Mo . Most diagnostic procedures involving radioactivity in the US involve $^{99}\text{Tc}^m$. Explain how you

would produce ^{99}Mo (the 66.0 hr parent of 6.0 h $^{99}\text{Tc}^m$). Consider two choices, production of ^{99}Mo as a fission product or via the $^{98}\text{Mo}(n,\gamma)$ reaction.

15. Calculate the activity of ^{254}No ($t_{1/2}=55$ sec) present 5 minutes after a 10 min irradiation of a 0.001 inch thick ^{208}Pb foil by ^{48}Ca projectiles ($\phi = 6.28 \times 10^{12}$ particles/sec). Assume $\rightarrow(^{48}\text{Ca}, 2n)$ is $3 \times 10^{-30} \text{ cm}^2$.

16. Consider the reaction $^{12}\text{C}(\alpha, n)$ where the laboratory energy of the incident projectile is 14.6 MeV. What is the excitation energy of the compound nucleus? The reaction cross section is 25 mb. Assuming a carbon target thickness of 0.10 mg/cm² and a beam current of 25 nA, compute the ^{15}O activity after a 4 min irradiation.

17. The cross section for the $^{60}\text{Ni}(\alpha, pn)$ reaction is 0.9 barn for 32 MeV α -particles. Calculate the number of disintegrations per minute of ^{62}Cu at 15 minutes after a 15 minute bombardment of a 50 mg/cm² foil of ^{60}Ni with 10 μA of 32 MeV α -particles.

18. Consider the reaction $^{29}\text{Si}(^{18}\text{O}, p2n)$ which populates the metastable and ground states of ^{44}Sc . Using the decay scheme shown below, and the fact that at EOB one observed 1000 photons/sec of energy 271.2 keV and 1000 photons/sec of energy 1157.0 keV, calculate the ratio of the cross section for the production of $^{44}\text{Sc}^m$, σ_m , to the cross section for the production of ^{44}Sc , σ_g . Neglect any decay of

$^{44}\text{Sc}^m$ to ^{44}Sc during the irradiation and assume the length of the irradiation was six hours.

